Chemical Science

ROYAL SOCIETY OF CHEMISTRY

REVIEW

View Article Online
View Journal | View Issue

Cite this: *Chem. Sci.*, 2025, **16**, 18535

Gas-mediated cancer therapy: advances in delivery strategies and therapeutic mechanisms

Jiaqi Yin,†[a] Jiarui Zhong,†[a] Wei Pan,[a] Yanhua Li,*[a] Na Li*[a] and Bo Tang[ab]

Gas therapy represents a novel anti-cancer strategy based on endogenous gas molecules. This approach offers several advantages over traditional therapies, including reduced drug resistance and enhanced tissue permeability, making it a prominent research focus in precise cancer treatment. To achieve effective gas therapy, researchers have developed increasingly innovative gas delivery systems and material platforms. Here, we review recent advances in gas therapy, especially those involving oxygen (O_2), carbon monoxide (CO), nitric oxide (NO) and hydrogen (H_2). We focus on introducing the cellular action mechanisms of various gases, newly developed methods for gas generation or transportation, and their main applications in cancer therapy. Moreover, the existing deficiencies in current strategies and the future development directions of gas-mediated cancer therapy are discussed.

Received 22nd July 2025
Accepted 22nd September 2025

DOI: 10.1039/d5sc05474e

rsc.li/chemical-science

1. Introduction

With the rapid progress of modern medicine, discovering a cure for cancer is a common aspiration for all humankind. Although surgery, chemotherapy, radiotherapy (RT), targeted therapy, and immunotherapy are widely used clinical treatments for cancer, their limitations including side effects and poor prognosis remain unavoidable. Surgery has limited efficacy against metastatic tumors and often causes severe surgical trauma.[1–3] Chemotherapy and RT lack specificity and cause serious damage to healthy tissues, resulting in a substantial decline in patients' quality of life.[4–6] Targeted therapy and immunotherapy face issues such as limited applicable populations, drug resistance, toxic side effects, and high treatment costs.[7,8] These challenges have driven scientists to continuously explore new anti-cancer strategies that are more precise, effective, and less toxic. Over the past few decades, various novel cancer treatments have emerged, including photodynamic therapy (PDT), photothermal therapy (PTT), chemodynamic therapy (CDT), sonodynamic therapy (SDT), and gas therapy. These methods typically act by generating reactive oxygen species (ROS), heat, or therapeutic gases to cause extensive damage and ultimately cell death in cancer cells. Regardless of the treatment strategy adopted, precise quantitative analysis of anti-cancer drugs is indispensable. Through techniques such as mass spectrometry, electrophoresis, spectroscopy and electrochemistry, the distribution and concentration of the drugs within the tumor site can

[a]*College of Chemistry, Chemical Engineering and Materials Science, Key Laboratory of Molecular and Nano Probes, Ministry of Education, Collaborative Innovation Center of Functionalized Probes for Chemical Imaging in Universities of Shandong, Institute of Molecular and Nano Science, Shandong Normal University, Jinan 250014, P. R. China. E-mail: liyanhua@sdnu.edu.cn; lina@sdnu.edu.cn*

[b]*Laoshan Laboratory, Qingdao 266237, P. R. China*

† These authors contributed equally.

Jiaqi Yin

Jiaqi Yin is currently pursuing a PhD degree at the College of Chemistry, Chemical Engineering and Materials Science at Shandong Normal University. Her current research interest is the detection of tumor markers and the design of functional nanomaterials for cancer therapy.

Jiarui Zhong

Jiarui Zhong is currently pursuing a Master's degree at the College of Chemistry, Chemical Engineering and Materials Science at Shandong Normal University. His current research interest is the design of small-molecule organic fluorescent dyes for disease imaging and therapy.

be monitored and evaluated.[9–14] These tools are of great significance for evaluating drug efficacy and improving drug effects.

Among these therapeutic approaches, gas therapy has rapidly become a cutting-edge hotspot in cancer treatment due to the unique tissue penetration and multi-target action mechanisms associated with gas molecules.[15–17] Gas therapy uses biologically active gas molecules, such as oxygen (O_2), carbon monoxide (CO), nitric oxide (NO), hydrogen (H_2), hydrogen sulfide (H_2S) and sulfur dioxide (SO_2) to kill cancer cells or enhance therapeutic efficacy by regulating the tumor microenvironment.[18–21] Compared with the first four gases, the two sulfur-containing gases have been developed relatively late in the field of cancer treatment, but their mechanisms are more complex and novel, requiring more in-depth introduction and discussion. Therefore, this review mainly focuses on the roles of O_2, CO, NO and H_2 in cancer therapy. Firstly, gas molecules are small in size and possess strong diffusion ability, allowing them to penetrate into deep tumor tissues. Secondly, since these gases are endogenously produced under physiological conditions, they cannot easily induce drug resistance. Thirdly, gas molecules can regulate tumor metabolism, the immune microenvironment, and cell death pathways through multiple mechanisms, providing promising avenues for overcoming resistance to traditional treatments.

O_2, CO, NO and H_2 have been shown to regulate cellular physiological functions and contribute to the treatment of various diseases. O_2 is essential for cellular energy supply and primarily inhibits tumor angiogenesis and metastasis by alleviating hypoxia.[19,22] NO and CO have been applied in the areas of anti-bacterial, anti-inflammatory and cardiovascular system regulation.[23–26] H_2 can serve as a therapeutic antioxidant and promotes wound healing.[27–29] In cancer therapy, the cellular mechanisms of gas action mainly include: (1) alleviating tumor hypoxia, (2) inducing mitochondrial dysfunction, (3) causing DNA damage, (4) aggravating oxidative stress, and (5) reversing multi-drug resistance (MDR).

For cancer treatment, improving drug delivery is one of the most important and effective ways to enhance efficacy and safety. Advanced drug delivery systems can precisely deliver drugs to the interior of tumor tissues by strengthening the enhanced permeability and retention (EPR) effect or through active targeting techniques and control their release behavior.[30–32] Although inhalation is the simplest way for gas therapy, the uncontrolled diffusion of gases limits their therapeutic efficacy. Therefore, a great deal of effort has been devoted to developing intelligent nanocarriers for accurate and controlled gas delivery to tumors.[17,33–35] In addition, some *in situ* gas generation strategies have been designed, which is another

Wei Pan

Wei Pan received his PhD in Analytical Chemistry from Shandong Normal University in 2014. Currently, he is a professor in the College of Chemistry, Chemical Engineering and Materials Science at Shandong Normal University. His research interests focus on the design and application of fluorescent nanoprobes.

Na Li

Na Li received her B.S. in 2004 and PhD in 2009 from Shandong University. After a postdoctoral fellowship at McMaster University, Canada, she joined Shandong Normal University in 2010. She became an associate professor in 2012 and was promoted to a full professor in 2014. Her research interests include the design and synthesis of functional nanoprobes for bioanalysis and cancer therapy.

Yanhua Li

Yanhua Li received her PhD in Analytical Chemistry from Shandong Normal University in 2020. Currently, she is a lecturer at the College of Chemistry, Chemical Engineering and Materials Science at Shandong Normal University. Her current research focuses on the tumor-microenvironment responsive nanomedicine of drug delivery systems and cancer immunotherapy.

Bo Tang

Bo Tang obtained his PhD in Analytical Chemistry in 1994 from Nankai University. Then he joined the College of Chemistry, Chemical Engineering and Materials Science as a full professor at Shandong Normal University. His current research interests include the development of molecular and nanoprobes for analytical and biomedical applications, solar energy chemical transformation and storage, and clean synthesis of chemicals.

major improvement in gas therapy.[17,36] Both approaches require the rational design of stimulus-responsive and targeted gas donors to minimize unwanted gas leakage during circulation and avoid off-target effects. To trigger intracellular gas release, endogenous stimuli like H^+, glutathione (GSH) and hydrogen peroxide (H_2O_2) and exogenous stimuli such as light, ultrasound and X-rays have been employed.[16,37] To broaden their applications, most gas therapeutic methods are conjugated with other anti-tumor treatments for mutual enhancement.[38] Moreover, gases can be employed in ultrasound imaging to monitor the gas generation process and therapeutic progression at the tumor site. It is worth emphasizing that such systems also play a crucial role in preventing environmental impact. Due to the introduction of precise delivery or generation methods, these methods can lower drug dosages and minimize environmental pollution, thereby facilitating the development of more sustainable treatment strategies. Furthermore, the relatively efficient drug utilization can reduce the reliance on secondary treatment methods such as photocatalytic degradation.[39–45]

In this review, we systematically summarize the anti-tumor capacities of O_2, CO, NO and H_2. We then highlight recent advances in gas delivery methods and gas-mediated cancer therapy strategies. Finally, we critically analyze current challenges in gas therapy and propose future research directions for this emerging field (Fig. 1).

2. O_2-mediated cancer therapy

Like food and water, O_2 is indispensable to the human body. It is the key substance in human metabolic activities and vital functions. However, hypoxia is one of the characteristics of most types of solid tumors. For example, the measured partial pressure of O_2 is < 2.5 mm Hg in breast cancer *versus* 65 mm Hg in normal breast tissue.[46] On the one hand, the high metabolic rate of cancer cells leads to excessive consumption of O_2 in tumor regions. On the other hand, the growing solid tumor tissues block and compress surrounding blood vessels, resulting in insufficient blood flow and O_2 supply. To adapt to this harsh living environment, cancer cells activate the hypoxia-inducible factor (HIF) signaling pathway to regulate downstream signal molecules and life activities for combating hypoxia.[46,47] Consequences of HIFs in cancer include inducing cell immortalization, metabolic reprogramming, abnormal angiogenesis, immune evasion and cancer invasion and metastasis.[47–49]

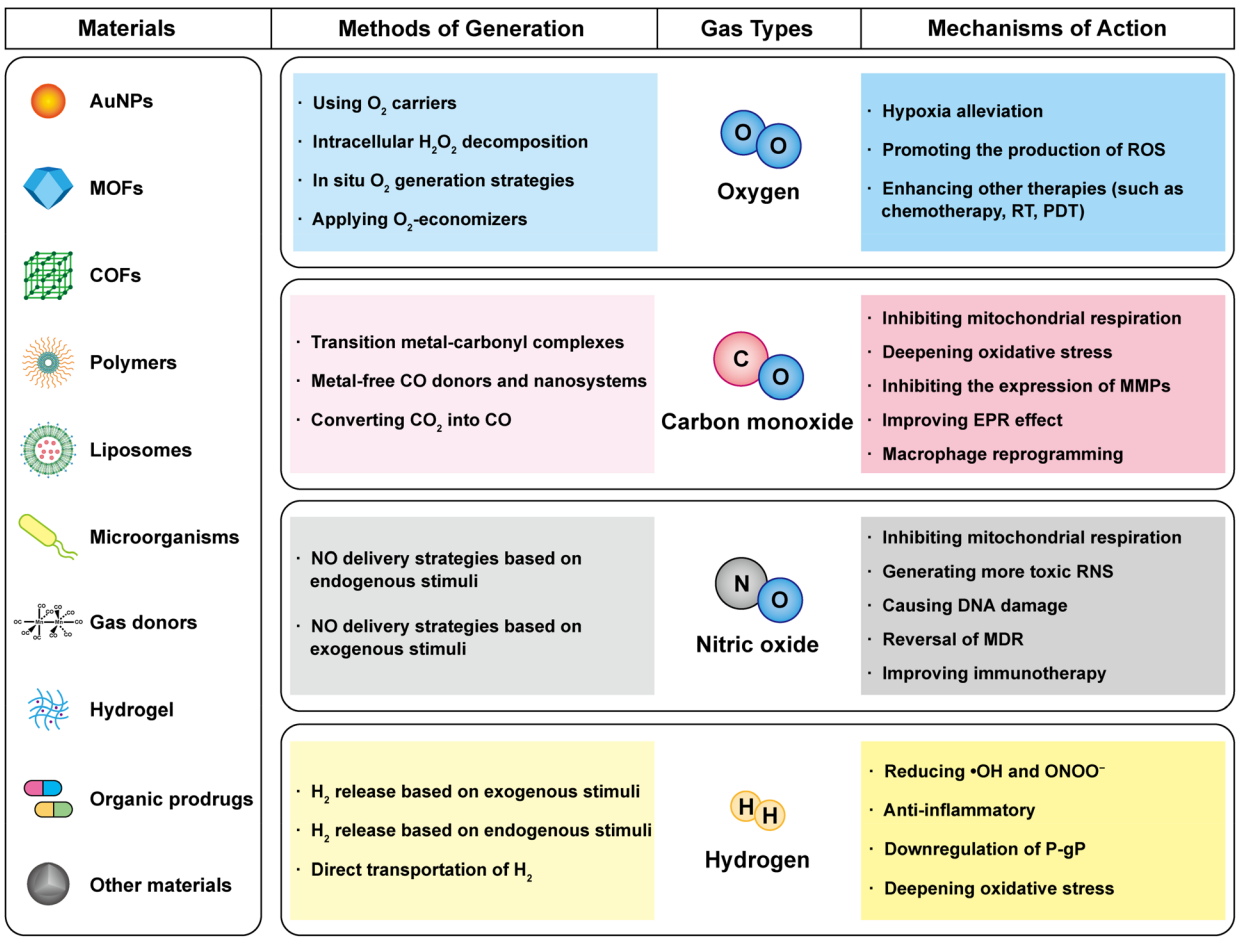

Fig. 1 Schematic illustration of gas-mediated cancer therapy, including the gas types, representative materials, methods of gas generation and mechanism of action.

Hypoxia is a major obstacle for most O_2-dependent cancer therapies, such as RT, PDT, CDT and SDT. Besides, it has been confirmed that hypoxia can increase the activity of permeability glycoprotein (P-gP) and enhance MDR of tumors.[49] In O_2-involved cancer therapies, O_2 itself is non-toxic to cancer cells, but it is mainly used to relieve the hypoxic microenvironment to assist other therapy strategies.

2.1 Using carriers for O_2 supply

The most direct way to increase the O_2 concentration inside the tumor is to deliver O_2 directly to tumor cells and alleviate hypoxia. Most of these strategies are based on O_2-carrying materials which can preload O_2 during chemical preparation and release O_2 after entering cells, thereby alleviating the hypoxic microenvironment.[50,51]

Among different kinds of O_2 delivery materials, perfluorocarbon (PFC) has prominent advantages due to its high O_2 solubility and good biocompatibility. Our group reported a chemiluminescence resonance energy transfer-based biomimetic nanoreactor for synergistic photodynamic-starvation therapy (Fig. 2A).[51] Hollow mesoporous silica nanoparticles (HMSNs) were modified with Ce6 and glucose oxidase (GOx) and then loaded with bis[2,4,5-trichloro-6-(pentyloxycarbonyl) phenyl] oxalate (CPPO) and PFC. In cancer cells, O_2 gradually escaped from PFC to modulate the hypoxic microenvironment. At the same time, GOx consumed glucose to produce H_2O_2, which further supplied substrates for ROS generation. Then CPPO reacted with H_2O_2 to generate high-energy intermediates and finally activated Ce6 to produce singlet oxygen ($^1O_2$), achieving non-light excited PDT. Yan's group reported novel nanoengineered acoustic neutrophils called "acouscyte/O_2" for SDT and multi-modal imaging of tumors.[52] Acouscyte/O_2 was composed of O_2-loading PFC, sonosensitizer temoporfin, tumor-targeting cRGD peptide modified liposomes and live neutrophils. Under ultrasound irradiation, acouscyte/O_2 could generate O_2 bubbles to relieve hypoxia in cancer cells. Temoporfin was demonstrated to act as a sonosensitizer for $^1O_2$ generation, and its function was still preserved in the hypoxic microenvironment due to the O_2 supplemented by PFC. Acouscyte/O_2 could downregulate the level of HIF-1α, promote ROS-induced cell apoptosis, and finally lead to tumor inhibition.

Recently, other highly fluorinated compounds or nanostructures have also been reported to carry O_2 in cancer therapies. Fang's group constructed a hybrid of a cancer cell membrane and thermosensitive liposomes as a carrier and

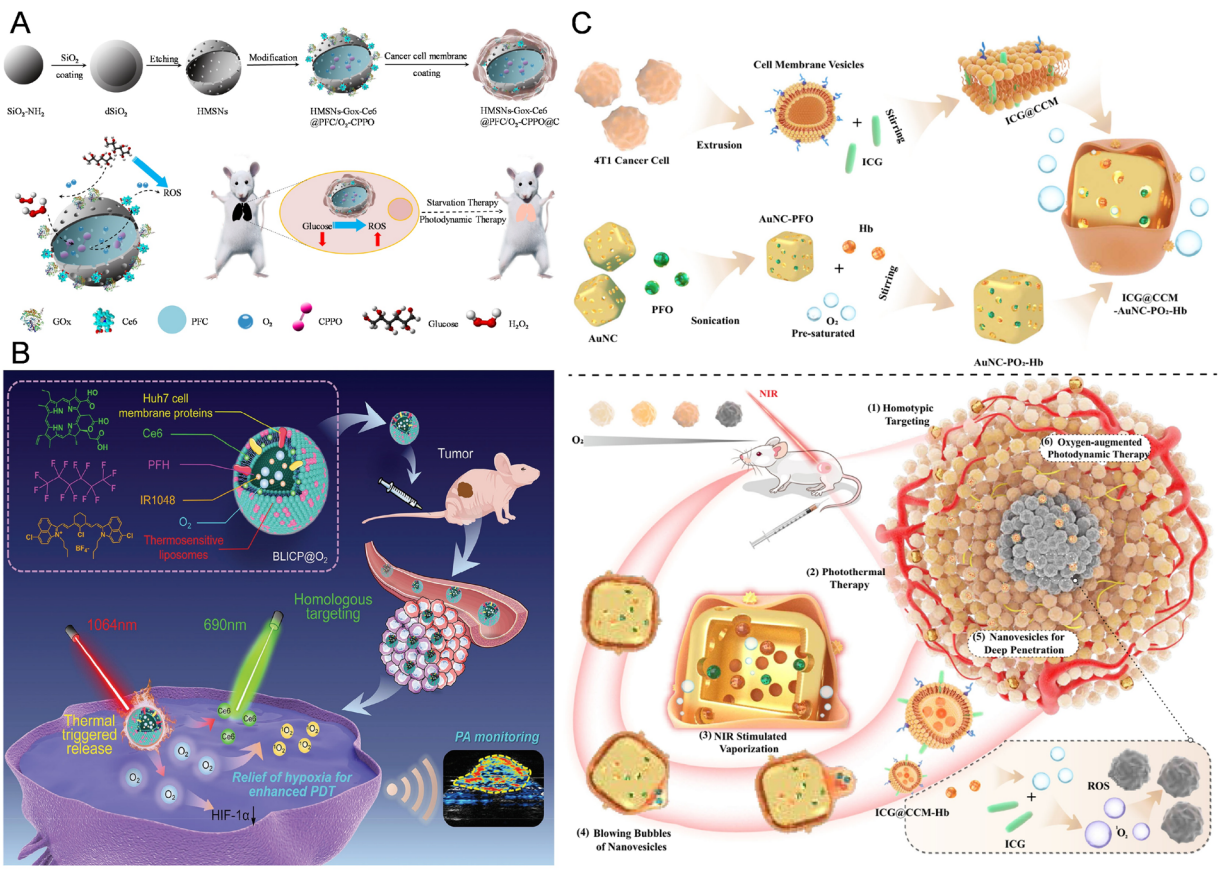

Fig. 2 O_2 carriers used for cancer treatment. (A) Schematic illustration of a biomimetic nanoreactor (HMSNs-GOx-Ce6@PFC-CPPO) and the mechanism of ROS production with no light irradiation in cancer cells. Reproduced with permission from ref. 51. Copyright 2018 Springer Nature. (B) The structure of BLICP@O_2 and the schematic illustration of intracellular O_2 supply and PDT. Reproduced with permission from ref. 53. Copyright 2024 Wiley-VCH GmbH. (C) The synthetic procedure and anti-tumor mechanism of ICG@CCM-AuNC-PO_2-Hb nanovesicles. Reproduced with permission from ref. 54. Copyright 2023 Springer Nature.

encapsulated IR1048 Ce6 and perfluorohexane (PFH) in it (Fig. 2B).[53] The heat generated under laser irradiation caused the O_2 carried in PFH to escape. The thermosensitive liposomes ruptured at the same time, which was conducive to the rapid diffusion of O_2. Tu's group aimed to squeeze cell membranes from biomimetic nanomaterials with heat-triggered PFH vapor to form bionic nanovesicles (Fig. 2C).[54] The nanovesicles were able to penetrate deeper tumor areas, deliver O_2 and achieve self-sufficient and O_2-boosted PDT. Feng's group chose octafluoropropane (C_3F_8) to fabricate microbubbles for O_2 supply and the relief of immunosuppressive microenvironments.[55] Besides, Fairen-Jimenez's group integrated perfluorooctyl segments with double-tailed phosphate-functionalized methoxy poly(ethylene glycol) to form F-PEG, which was grafted onto metal–organic frameworks (MOFs), exhibiting excellent O_2-carrying capacity.[56] Liu's group designed fluorocarbon-chain-functionalized hollow mesoporous organosilica nanoparticles (FHMONs) for sonodynamic treatment of pancreatic cancer.[57] Fluorocarbon chains exhibited strong affinity toward O_2 and were easier to use and more stable to store, which made them an ideal alternative to PFC.

2.2 Intracellular H_2O_2 decomposition for O_2 supply

Exogenous O_2 carriers may be limited by the complex physiological barriers of tumors, making it difficult for O_2 to be delivered efficiently and precisely to the most critical areas with hypoxia. Moreover, unexpected leakage during the delivery process can also lead to insufficient effects. Therefore, using endogenous O_2 donors, such as H_2O_2, provides a good alternative method.

H_2O_2 is a strong oxidizing agent, and its redox potential is +1.78 V.[58–60] Its decomposition rate depends on efficient catalysts (such as nanoenzymes) to achieve rapid O_2 generation required for treatment, and it has both safety and potential for synergistic treatment. Given the elevated levels of oxidative stress and overexpressed H_2O_2 in cancer cells, decomposition of H_2O_2 into O_2 is an effective approach. Many substances with catalytic activity have been used to build materials for H_2O_2 decomposition, such as MnO_2, Fe^{3+}, Ru, Prussian blue, CeO_2 and catalase (CAT).

As one of the non-invasive treatment methods, PDT has been applied clinically for treating localized tumors and other diseases because of the controllable temporal and spatial light irradiation and relatively mild side effects. Unfortunately, vascular malformation and excessive O_2 consumption in tumor hypoxic regions seriously hinder ROS production, resulting in limited application of PDT. Thus, many researchers combined H_2O_2 decomposition with PDT as an ideal approach to solve this problem. For example, Lo's group proposed novel Fe^{3+}-promoted PDT nanozymes (Fmoc-Cys/Fe@Pc/ACF), which could release Fe^{3+} ions to react with H_2O_2 and release O_2, aiming to reverse the inefficient therapeutic effect caused by hypoxia.[61] Hyeon's group constructed mesoporous silica nanoparticles anchored by manganese ferrite nanoparticles (MFMSNs) and loaded with chlorin e6 (Ce6). As CAT-like agents, MFMSNs exerted their ability to catalyze H_2O_2 into O_2 consistently and assisted Ce6-mediated PDT (Fig. 3A).[62] Shi's group constructed a synergistically augmented immunometabolic anti-cancer strategy, which included O_2 production from CAT-catalyzed H_2O_2 decomposition, Ce6-mediated cytotoxic $^1O_2$ generation and NLG-919-induced 2,3-dioxygenase inhibition.[63] Upon 660 nm laser irradiation, the nanocapsule played a role in ROS generation and immune response activation, resulting in synergistic photodynamic and immunometabolic therapy. Zhao's group reported a novel single-atom enzyme (OxgeMCC-r SAE) with rapid O_2 generation velocity (Fig. 3B).[38] The tumor hypoxia reversal can be attributed to six unsaturated coordination sites of Ru–C_6, which had a catalytic reaction rate of 0.041 min^{-1}, much faster than that of the widely used MnO_2 (0.029 min^{-1}). OxgeMCC-r SAE possessed significant intracellular O_2 production and enhanced PDT efficiency, which were further evaluated using PDT therapy results. Shen's group loaded aggregation-induced emission (AIE) molecules with photothermal and photodynamic therapeutic capabilities into a Prussian blue nanocatalyzer (Fig. 3C).[64] This design leveraged Prussian blue's ability to catalyze O_2 production in the tumor microenvironment for improving the PDT effect. Besides, $Ti_2C(OH)_2$ nanosheets, ruthenium metal complexes and two-dimensional (2D) layered double hydroxide (LDH) nanosheets have also been reported to decompose H_2O_2 and relieve the hypoxic microenvironment in PDT.[65–67]

In addition to PDT, O_2 also helps in the implementation of RT, chemotherapy and mRNA vaccine-based therapy. For instance, Chen's group reported a multi-sensitized radiotherapy strategy based on 2D graphdiyne–CeO_2 nanocomposites and miR181a.[68] Ce^{4+} ions in CeO_2 NPs were reduced to Ce^{3+} and decomposed H_2O_2 to release O_2 for hypoxia reversal. Gao's group constructed PTX/ICG-NVs@Au@CAT nanoparticles for synergistic photodynamic, photothermal, chemo- and immunotherapy.[69] With the assistance of CAT, hypoxia relief not only broke the chemoresistance of cancer cells, but also provided enough raw materials for ICG to generate more ROS. As for the nanomRNA vaccine, Yu's group used lipids to wrap Mn_3O_4 nanoparticles and antigen encoding mRNA to prepare nanovaccines (MnLNPs) (Fig. 3D).[70] MnLNPs could eliminate ROS and catalyze the decomposition of H_2O_2. The production of O_2 promoted the synthesis of ATP, enhanced mRNA translation, and effectively improved the activation efficiency of the cGAS-STING pathway.

Furthermore, in order to increase the concentration of H_2O_2, the delivery strategies of H_2O_2 have been improved to a certain extent and been applied in ferroptosis therapy, radioimmunotherapy, and other fields. These strategies can also be combined with O_2-mediated cancer treatments to achieve better results.[71,72]

2.3 *In situ* O_2 generation strategies

Although significant progress has been made in strategies for directly delivering O_2 through carriers or catalyzing the decomposition of endogenous H_2O_2, they are usually limited by the physiological barriers of tumors and their dependence on the concentration of H_2O_2 at the tumor site. To overcome these

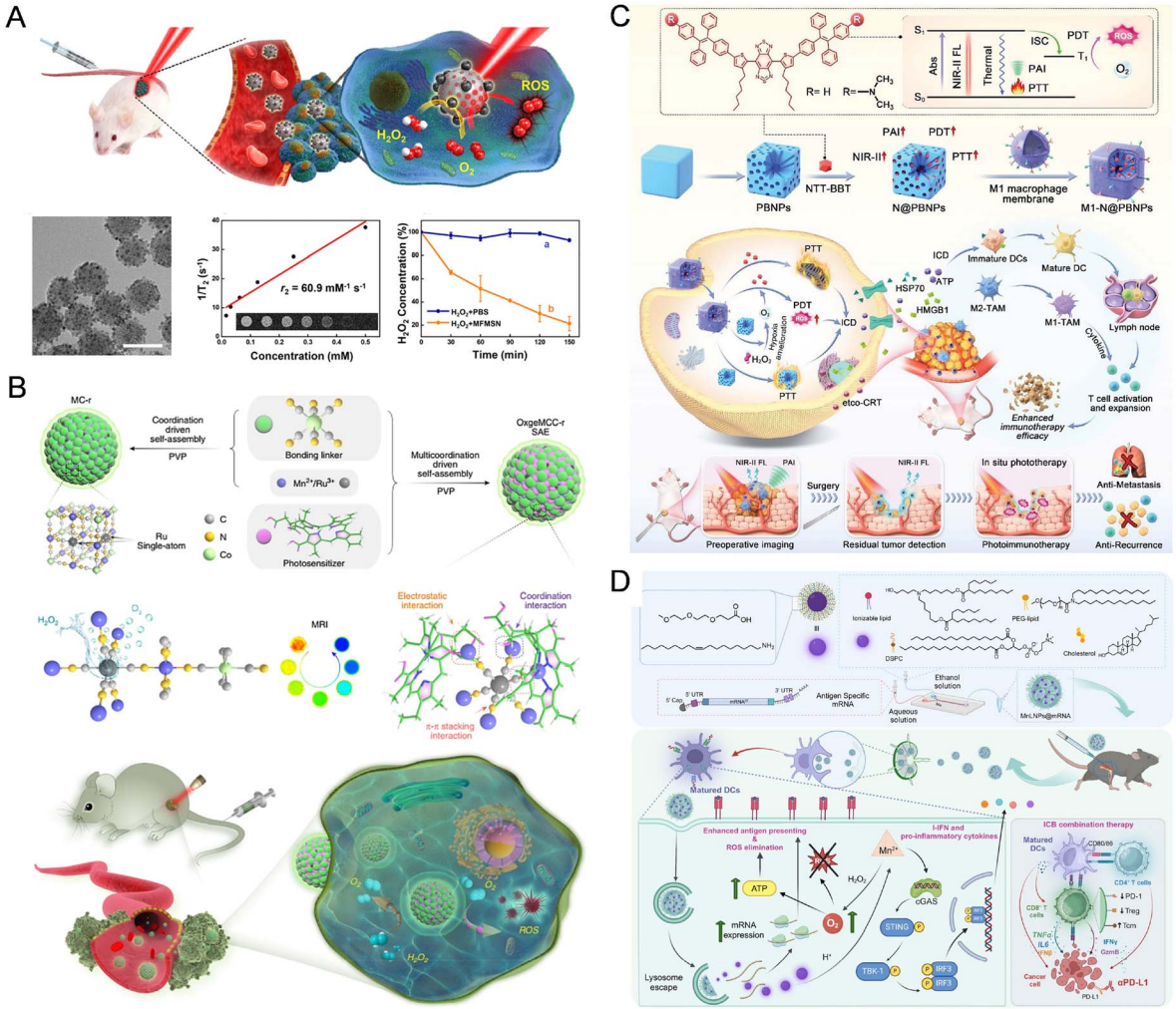

Fig. 3 H_2O_2 decomposition strategies for O_2 supply. (A) Schematic illustration, electron microscopy image, T2-weighted magnetic resonance imaging ability and H_2O_2 decomposition ability ((a): H_2O_2 + PBS; (b): H_2O_2 + MFMSNs) of MFMSNs. Reproduced with permission from ref. 62. Copyright 2017 American Chemical Society. (B) The preparation process, active single-atom Ru sites and intracellular PDT capability of OxgeMCC-r nanozymes. Reproduced with permission from ref. 38. Copyright 2020 Springer Nature. (C) Schematic illustration of an AIEgen-loaded Prussian blue nanocatalyzer for O_2 generation and robust cancer therapy. Reproduced with permission from ref. 64. Copyright 2024 Wiley-VCH GmbH. (D) The preparation process and mechanism of action of the MnLNPs@mRNA vaccine. Reproduced with permission from ref. 70. Copyright 2024 American Chemical Society.

limitations, more autonomous *in situ* oxygen generation strategies have been developed.

Some inorganic materials with water splitting abilities have been used to develop O_2 generation strategies. For example, CaO_2 can react with H_2O to generate $Ca(OH)_2$, H_2O_2 and O_2. Thus, numerous *in situ* O_2 generation strategies based on it have been proposed.[36,73,74] Dong's group designed a H_2O_2/O_2 self-supplying nanosystem ((MSNs@CaO_2-ICG)@LA) for combined PDT and CDT (Fig. 4A).[74] Sung's group developed a kind of O_2-generating depot to overcome hypoxia-induced resistance to DOX in chemotherapy, where CaO_2 and CAT both contributed to abundant O_2 generation.[36] C_3N_4 has also been introduced to supply O_2 owing to its ability to split H_2O. For example, Yin's group conjugated C_3N_4 nanosheets onto a catalytic therapy/PTT system for *in situ* O_2 generation (Fig. 4B).[75]

Besides, some microorganisms with O_2-producing capacity may provide new O_2 delivery conceptions. For instance, Ce6 was modified by Shi's group to expose positively charged amino groups and then incubated with cyanobacterial cells to construct photosensitive and photosynthetic cyanobacteria for O_2 generation and $^1O_2$ conversion.[76] Under 660 nm laser irradiation, the hybrid ceCyan cells not only produced a large amount of O_2 to reverse the low efficiency of PDT caused by hypoxia, but also delivered Ce6 into tumor cells for the following $^1O_2$ generation. This kind of novel O_2 manufacturer and photosensitizer reservoir pool has provided a new idea for overcoming the hypoxia environment in type II PDT.

2.4 Applying O_2-economizers to combat hypoxia

Apart from the above three methods of increasing O_2 content through "open sources", "throttling" is also a way to enhance the intracellular O_2 concentration.

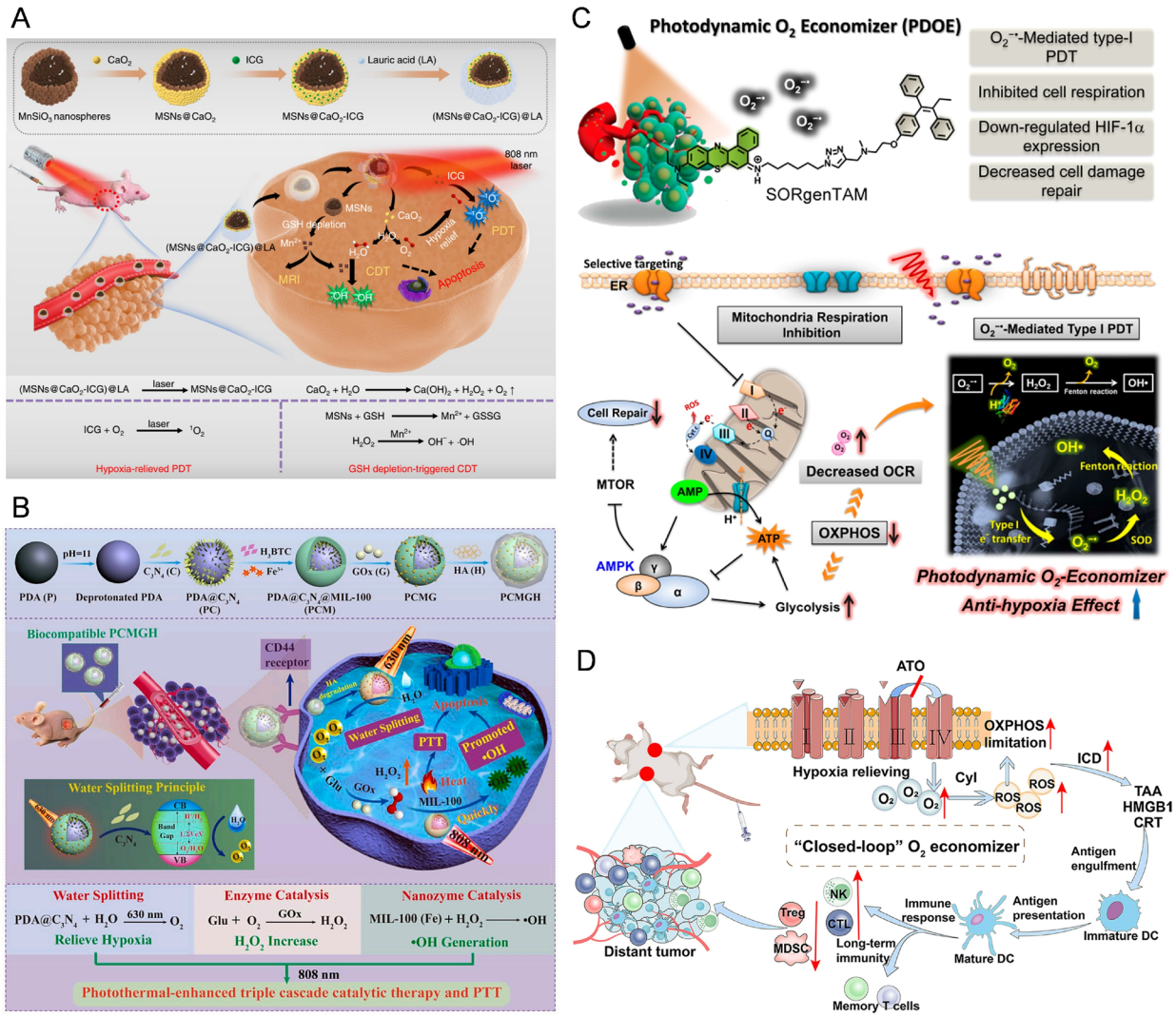

Fig. 4 Intracellular O_2-generators and O_2-economizers. (A) Schematic illustration of (MSNs@CaO_2-ICG)@LA NPs. The nanoparticles were able to deplete GSH and relieve hypoxia to assist CDT and PDT. Reproduced with permission from ref. 74. Copyright 2020 Springer Nature. (B) The synthesis process and mechanism of action of a C_3N_4/nanozyme/GOx triple cascade nanocatalyst. Reproduced with permission from ref. 75. Copyright 2021 Elsevier Ltd. (C) Schematic illustration of a photodynamic O_2-economizer (SORgenTAM). Reproduced with permission from ref. 77. Copyright 2020 American Chemical Society. (D) Schematic illustration of an O_2-economizer (TPCA) for a PDT-induced *in situ* vaccine. Reproduced with permission from ref. 78. Copyright 2023 American Chemical Society.

Recently, some researchers focused on decreasing intrinsic O_2 consumption rather than increasing O_2 supply and put forward an "O_2-economizer" concept to overcome the hypoxia barrier. Peng's group designed SORgenTAM for enhanced PDT of hypoxic tumors, taking advantage of tamoxifen-induced mitochondrial metabolic disorder (Fig. 4C).[77] By inhibiting O_2 consumption from cancer cell respiration, the saved endogenous O_2 could be used to generate more ROS, which opened a new window for the reversal of hypoxia-triggered PDT tolerance. Similarly, Cao's group chose atovaquone, an inhibitor of mitochondrial oxidative phosphorylation (OXPHOS), to fabricate an O_2-economizer (TPCA), which was also verified to cause disruption of the electron transport chain and decrease O_2 consumption (Fig. 4D).[78] Hou's group synthesized DSPE-SS-PEG2k@TPP@TCPP@DPA-MOF nanoparticles to destroy the mitochondrial OXPHOS pathway and alleviate tumor hypoxia, which was mainly dependent on $^1O_2$ produced by TCPP under laser irradiation.[79] To better relieve hypoxia, You's group prepared $Ti_2C(OH)_2$ nanosheets with Ce6 to fabricate $Ti_2C(OH)_2$–Ce6.[67] At acidic tumor sites, $Ti_2C(OH)_2$ nanosheets combined with phosphorylated proteins to inhibit mitochondrial respiration and catalyze endogenous H_2O_2 to generate O_2. Compared to simply producing O_2 or reducing O_2 consumption, this strategy provided a more comprehensive approach.

It can be seen from the above research that O_2 occupies an important position in the field of gas therapy. However, these materials still have issues of insufficient safety and low utilization rate. Therefore, materials used in O_2-mediated cancer treatment must undergo strict evaluation, and the design of the materials should be simplified as much as possible to reduce possible risks.

3. CO-mediated cancer therapy

CO, a colorless and odorless carbon–oxygen compound, is gaseous at room temperature. Endogenous CO in humans is mainly produced by heme oxygenase (HO) metabolism and can bind with hemoglobin to form carboxyhemoglobin (COHb).[80] Under normal circumstances, the content of COHb in blood is about 0.5–0.8%.[81] However, owing to the much higher affinity of CO for hemoglobin than O_2, massive inhalation of CO can block O_2 delivery, causing systemic hypoxia and even cell death, which is called "CO poisoning".[82] Although CO has been considered an air pollutant and a toxic substance for a long time, more and more researchers have recognized the significance of CO in human health including anti-inflammatory, antibacterial, anti-cancer, central nervous system function regulation and cardiovascular system function regulation.[26,82–85]

For cancer therapy, the effects of CO can be summarized as follows. Firstly, high concentrations of CO mainly act on the electron transport chain and inhibit the function of cytochrome c oxidase. Redundant electrons escape and directly react with O_2 to induce massive ROS production, leading to mitochondrial damage and the disruption of ATP supply.[82,86,87] Secondly, CO inhibits the enzymatic activity of cystathionine β-synthase and decreases the level of GSH, thus disrupting redox homeostasis and deepening oxidative stress.[88] Thirdly, CO-induced ROS overproduction triggers the transformation of macrophages from the M2 phenotype to the M1 phenotype, which helps the immune system to recognize and kill cancer cells.[82] In addition, the expression of matrix metalloproteinases (MMPs) is inhibited by CO so that the progression and metastasis of tumors become more difficult.[89,90] Finally, CO may increase vascular permeability and strengthen the EPR effect for drug accumulation in solid tumors.[91]

To completely leverage the anti-cancer effect of CO, the foremost challenge is achieving precise delivery. Direct inhalation of CO gas is simple and fast, but it cannot guarantee the metrological controllability and targeted selectivity. Therefore, controllable CO donors and CO delivery nanoplatforms have always been the focus of research. In 2002, Motterlini *et al.* first reported a series of transition metal carbonyls as carbon monoxide releasing molecules (CORMs), including $Fe(CO)_5$, $Mn_2(CO)_{10}$ and $[Ru(CO)_3Cl_2]_2$.[92] Since then, a variety of CORMs have been extensively studied and applied in cancer therapy.[93,94] Moreover, many modified CORMs, metal-free CO prodrugs and *in situ* CO generation strategies have been reported recently, which greatly promote the development of CO-mediated gas therapy of cancer.[95,96]

3.1 Transition metal-carbonyl complexes as CO donors

Most metal-based CO donors are transition metal-carbonyl complexes, composed of transition metal centers and carbonyl ligands. Under stimulations, such as ROS, pH, heat and light, these CORMs will undergo ligand dissociation to release CO.

$Mn_2(CO)_{10}$, also termed MnCO or CORM-1, has been employed in many CO-mediated cancer therapy strategies. CO releasing from $Mn_2(CO)_{10}$ can be triggered by heat. For example, Chen's group synthesized HMOPMs-CO for specific CO delivery and synergistic PTT of glioblastoma.[97] On the one hand, lower pH would lead to the protonation of Mo(VI)-based polyoxometalate inside nanoparticles, causing the self-assembly and accumulation of HMONs at the tumor site. On the other hand, GSH would reduce Mo(VI) to Mo(V) and enhance the PTT performance of HMOPM-CO, which further induced the photothermal-controlled CO release from hydrophobic $Mn_2(CO)_{10}$ molecules. Therefore, HMOPMs-CO exhibited excellent tumor synergistic therapeutic efficacy in the mild acidic and GSH-enriched TME. Fan's group also used photothermal conversion in CO production from $Mn_2(CO)_{10}$ (Fig. 5A).[98] To decrease nonradiative decay and increase near-infrared region II (NIR-II) fluorescence intensity, they applied an "electron acceptor density adjustment" strategy to vary the density of electron withdrawing molecule TTQ and synthesized a series of conjugated copolymers. Among eight new structures, TTQ-2TC-4T was selected as the optimal NIR-II photothermal agent to induce the release of CO by breaking the Mn–CO bond in $Mn_2(CO)_{10}$. At tumor sites, high concentrations of CO caused mitochondrial dysfunction and promoted the generation of ROS. Finally, *in vitro* and *in vivo* experimental results confirmed the synergistic therapy effect resulting from the combination of CO, ROS and heat. Apart from heat, CO releasing activity of $Mn_2(CO)_{10}$ is also sensitive to H_2O_2.[89,99–101] For example, Song's group selected GOx to produce H_2O_2, and then MnCO was reacted with H_2O_2 to release CO for gas therapy.[100] To overcome the limited level of endogenous H_2O_2 and realize more efficient CO release, Gao's group used ionic liquids to form photogenerated holes and oxidase water to produce more H_2O_2 for CO release from $Mn_2(CO)_{10}$ (Fig. 5B).[101] Then $Mn_2(CO)_{10}$ was oxidized to MnO_2, which could induce more ROS and deplete glutathione. Therefore, the redox homeostasis was severely disrupted, eventually leading to cell apoptosis.

Based on another manganese carbonyl complex, $MnBr(CO)_5$, some anti-cancer nanoparticles are constructed to employ combined RT and CO therapy. For example, Liu's group designed a CO-releasing nanomicelle system (GW/MnCO@PLGA).[102] GdW_{10} nanoparticles were used for X-ray-excited ROS generation (such as superoxide anion ($O_2^{\bullet-}$)). Then, $O_2^{\bullet-}$ competed with the Mn center, causing Mn–CO bond breaking and CO release on demand. Under the synergistic effect of CO and $O_2^{\bullet-}$, the DNA repair process of cancer cells was impaired and resulted in effective killing of cancer cells. In addition, CORM-401 and CORM-$C_{30}H_{49}N_3Mn(CO)_3Br$ have also been reported for CO release in cancer therapies.[93,94]

Apart from Mn, Fe is also widely used as the center of carbonyl complexes. Ye's group designed a nano-sonosensitizer (AIBA@FeCuS–FeCO) with ultrasound-activated CO release and cell ferroptosis capacities for the ablation of deep gastric tumors.[103] Here, $Fe_3(CO)_{12}$, as a kind of radical-sensitive CO donor, was encapsulated in lipid nanoparticles and responded to AIBA radicals generated upon ultrasound irradiation. CO liberated from donors was effective in promoting blood flow and enhancing the EPR effect. Gong's group combined $Fe_3(CO)_{12}$, mPEG2000-SH and PBPTV to synthesize an

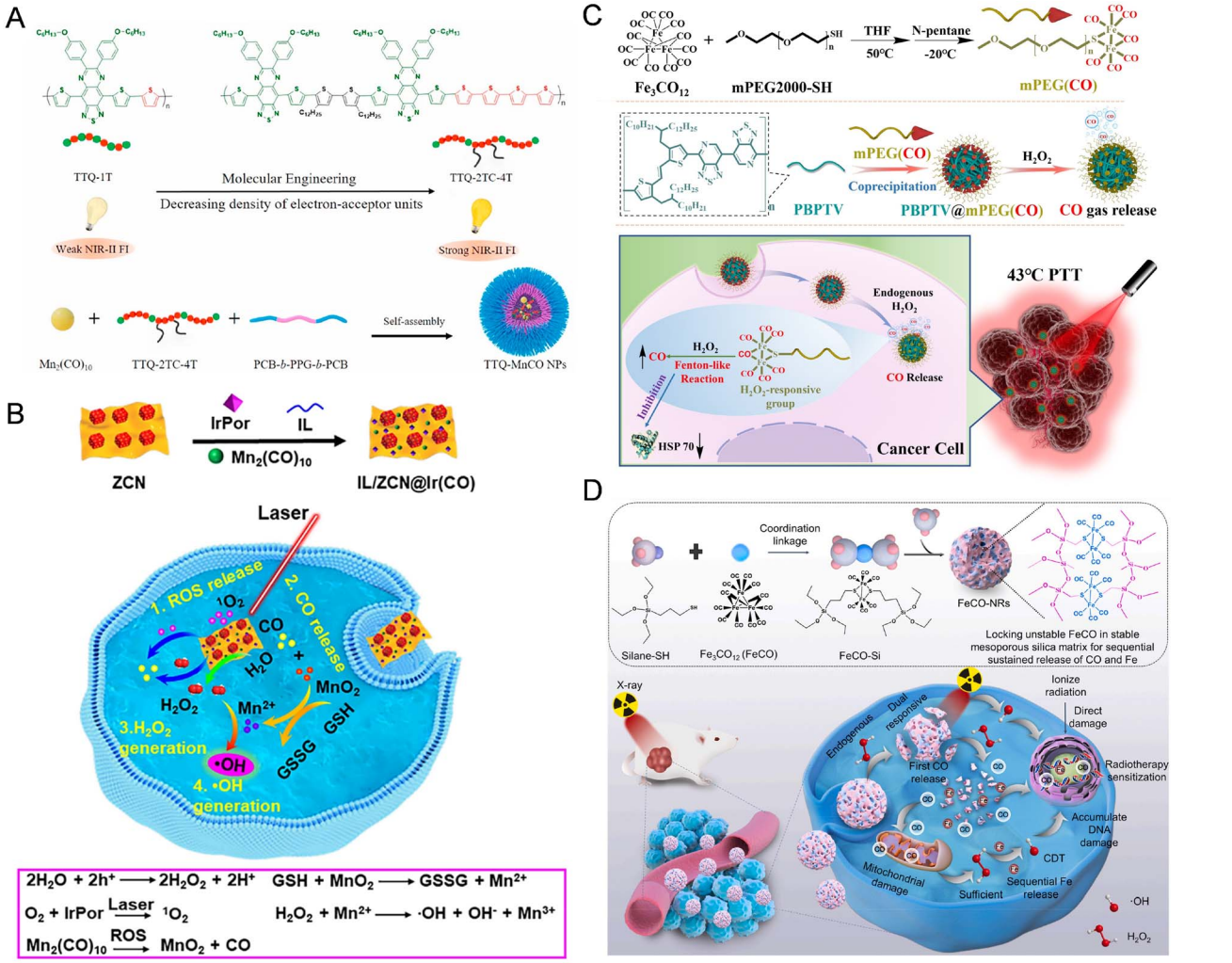

Fig. 5 CO donors based on transition metal-carbonyl complexes. (A) Chemical structure of TTQ-2TC-4T and the preparation process of TTQ-MnCO NPs. Reproduced with permission from ref. 98. Copyright 2021 Elsevier Ltd. (B) Schematic illustration of IL/ZCN@Ir(CO) and the process of the generation of CO and ROS. Reproduced with permission from ref. 101. Copyright 2024 American Chemical Society. (C) Schematic illustration of PBPTV@mPEG(CO). After entering tumor cells, PBPTV@mPEG(CO) could be decomposed by endogenous H_2O_2 and release CO to assist low-temperature PTT. Reproduced with permission from ref. 104. Copyright 2022 Wiley-VCH GmbH. (D) The synthesis process of FeCO-NRs and its anti-tumor mechanism. Reproduced with permission from ref. 106. Copyright 2023 Elsevier Ltd.

endogenous H_2O_2-responsive nanobomb for CO-augmented low-temperature PTT (Fig. 5C).[104] In the presence of higher levels of H_2O_2 in 4T1 cells, the nanobomb rapidly released CO from the carbonyl complex, while no obvious CO release happened in normal cells, confirming H_2O_2-triggered Fe–CO bond cleavage. Notably, western blotting assay results indicated that CO could down-regulate the intracellular HSP70 level, which might be one of the main reasons to explain the enhanced performance of low-temperature PTT (43 °C) caused by CO. In the work of Zhang's group, $Fe(CO)_5$ was encapsulated into the cavity of a Au nanocage.[105] Under NIR irradiation, $Fe(CO)_5$@Au was decomposed to Fe and CO. The accumulation of CO induced mitochondrial damage and jointly caused a ROS burst with Fe^{2+}. These changes together led to intracellular autophagy, autolysosome destruction and 4T1 cell death. Pei's group synthesized an FeCO-conjugated organosilane precursor *via* the coordination between $Fe_3(CO)_{12}$ and silane-SH and then constructed FeCO-bridged nanoreservoirs (FeCO-NRs) using a modified sol–gel method (Fig. 5D).[106] FeCO-NRs were much more stable and less likely to cause unwanted CO leakage and Fe^{2+} release.

Moreover, the application of rhenium (Re) carbonyl complexes in cancer inhibition has been developed for some time. Zhang's group reported a cyanine-linked Re carbonyl complex (Re-Cy) as the CO donor with enhanced sonosensitivity for SDT and CO-mediated gas therapy.[107] Notably, the more efficient CO-releasing performance came down to the enlarged π–π conjugate plane after cyanine moieties' conjugation. The more obvious depletion of GSH and downregulation of GPX4 indicated the stronger ferroptosis induced by Re-Cy than the original Re-CHO molecule. Besides, Huo's group selected a Re-centered CORM as a CO donor and ruthenium (Ru)-complex as a photosensitizer to synthesize a RR polymer, which further self-assembled to RR nanoparticles.[108] Under light irradiation, the

Ru-complex was excited to generate ROS to break the Re–CO bond and release CO, thereby achieving light-regulated PDT and gas therapy.

3.2 Metal-free CO donors and nanosystems

Although plenty of transition metal-based CORMs have been established and helped people to understand the mechanism of CO-involved gas therapy, the biological incompatibility, metabolic pathway and potential hazards of metal-based CORMs restrict their application. The development of metal-free CO donors and delivery systems may provide us with new perspectives.

3-Hydroflavone (3-HF), a candidate for CORMs, can precisely and controllably release CO under light irradiation. More importantly, the decomposition products (such as 2-(benzoyloxy)benzoic acid) and other derivatives of 3-HF exhibit low toxicity. On this basis, Xu's group combined HepG2 cell and red blood cell membranes to synthesize biomimetic nanocarriers of DOX and 3-HF.[109] Red light-triggered CO generation significantly enhanced the therapeutic effect of DOX, increasing the inhibition rate from 29% to 82.4%.

In recent years, Ji's group focused on developing metal-free CORMs. In 2022, their group designed a new type of metal-free CO donor (FL3) and devised a H_2O_2-responsive CO delivery polymer prodrug based on photo-decaying chemistry (Fig. 6A).[110] CO was generated through 3 steps: (1) endogenous H_2O_2 reacted with oxalate ester in polymer drugs to form a highly activated intermediate; (2) the activated intermediate transferred its energy to FL3 encapsulated in the polymer; (3) FL3 was activated after back electron transfer and released CO

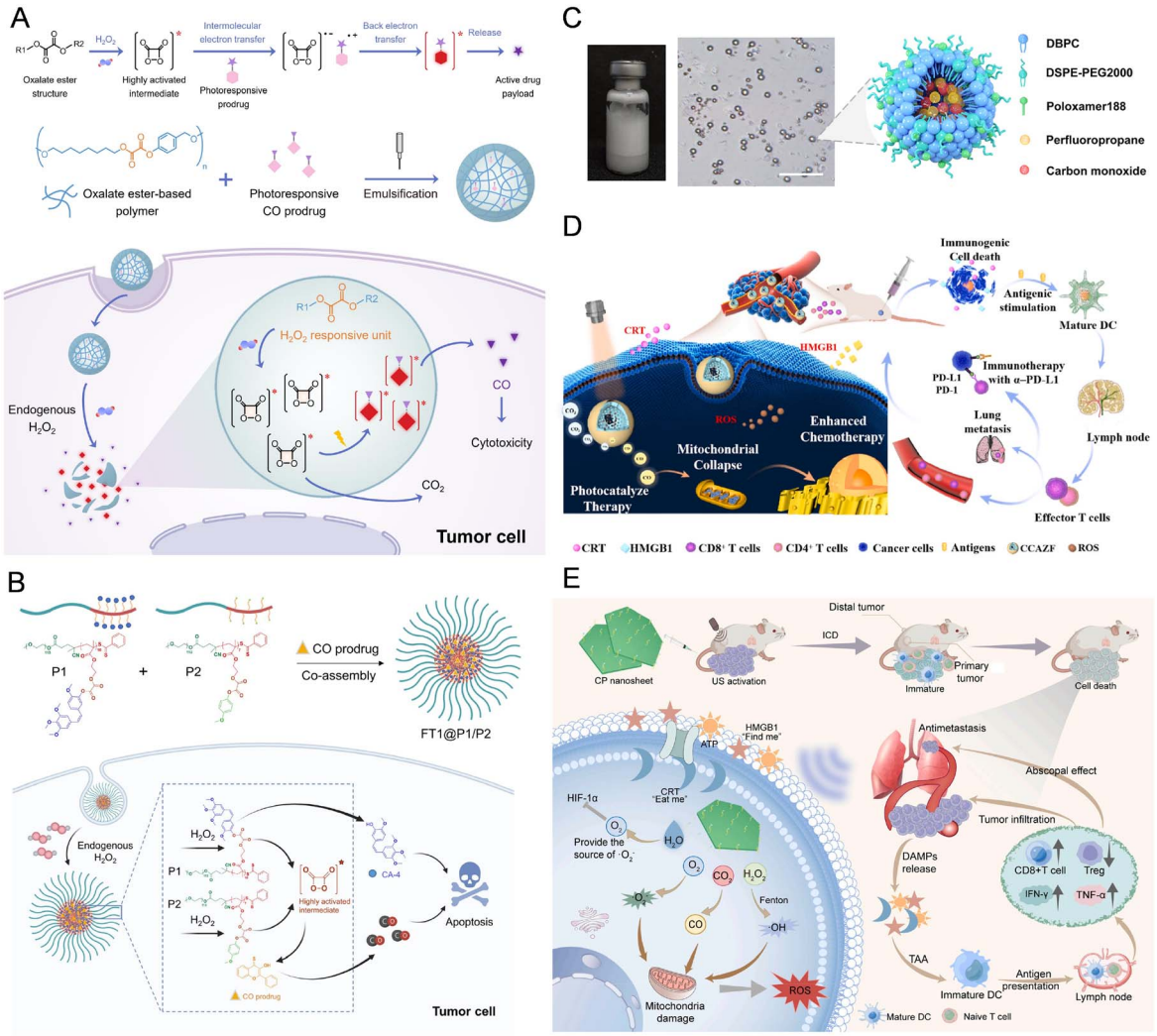

Fig. 6 Metal-free CO donors and CO_2 conversion strategies. (A) Schematic illustration of photoresponsive and metal-free CO donors. Reproduced with permission from ref. 110. Copyright 2022 Wiley-VCH GmbH. (B) The structure of an FT1@P1/P2 poly-prodrug nanosystem and its mechanism of action in tumor cells. Reproduced with permission from ref. 112. Copyright 2025 Science China Press. (C) The image, micrograph and structural schematic diagram of TARC-COs. Reproduced with permission from ref. 113. Copyright 2022 American Chemical Society. (D) Schematic illustration of CCAZF with anti-PD-L1 for converting CO_2 into CO and cancer immunotherapy. Reproduced with permission from ref. 116. Copyright 2021 Elsevier Ltd. (E) Schematic illustration of CP nanosheets and the process of inducing ICD. Reproduced with permission from ref. 117. Copyright 2023 Elsevier B.V.

in tumor cells. Later, a kind of metal-free CORM designed by them was able to release CO in response to multiple ROS including H_2O_2, $ONOO^-$ and ClO^-.[111] *In vitro* and *in vivo* anticancer experiments indicated that the therapeutic effect of these CORMs was related to the CO release rate. 3-Hydroxyflavothione (FT1), another kind of metal-free CORM, possessed higher CO release quantum yield than 3-HF. Recently, their group proposed a chemiexcitation-triggered prodrug activation strategy based on FT1 (Fig. 6B).[112] In response to intracellular H_2O_2, the FT1@P1/P2 poly-prodrug nanosystem could release CO and chemotherapeutic drug CA-4 effectively at the tumor site to carry out synergistic chemotherapy and gas therapy.

Unlike traditional organic or inorganic small molecule gas donors, microbubbles can directly load gases inside and release them under ultrasound pressure. Inspired by this method, Zhang's group synthesized ultrasound-triggered microbubbles (TARC-CO) as carriers of CO (Fig. 6C).[113] DBPC, DSPE-PEG2000, and poloxamer188 were mixed to form a microbubble shell and C_3F_8 gas was blended with CO gas as the core to improve the stability of TARC-COs. Owing to the excellent loading capacity of microbubbles, up to 337.1 ± 8.0 ($\times 10^3$ ppm) of CO was encapsulated in the unit volume of TARC-CO suspension. The CO releasing behavior of TARC-CO could be precisely controlled by the timing and position of ultrasound irradiation. *In vitro* and *in vivo* experimental results verified the targeted CO gas delivery and satisfactory therapy effect on 4T1-tumors.

3.3 Converting CO_2 into CO

Despite the fast development in metal-based or metal-free CORMs, researchers have to face the risk of unwanted CO leakage and potential toxicity due to hemoglobin binding. The partial pressure of CO_2 in tumor tissues is approximately 80 mmHg, much higher than that in normal tissues.[114] This concentration difference mainly results from elevated bicarbonate ion concentrations and the lower pH value within tumor cells. Besides, the concentration of CO in most CO-mediated cancer treatments is at the μM level, so the concentration of CO_2 is sufficient to meet the requirements for CO production.[15]

In recent years, reducing endogenous CO_2 to CO at the tumor site has emerged as a promising strategy for achieving more controllable and safer CO-mediated gas therapy. The reduction of CO_2 can be triggered by light or ultrasound using appropriate catalytic materials.

For example, Zhang's group functionalized partially oxidized SnS_2 nanosheets (POS NSs) with a tumor targeting polymer (PEG-cRGD) and loaded DOX onto the nanosheet to prepare PPOSD.[115] The POS moiety in PPOSD reduced CO_2 to CO under 561 nm laser irradiation and served as a PTT agent for tumor ablation under 808 nm laser irradiation. In this system, CO could not only cause damage to mitochondrial function, but also relieve local inflammation caused by PTT. Besides, they prepared HisAgCCN nanomaterials to provide CO *via* photocatalysis under 630 nm laser irradiation for targeted 4T1-tumor inhibition.[114] They found that CO could enhance the sensitivity of tumor cells to chemotherapy drug DOX and protect normal cells from chemotherapy, thus enhancing the safety and efficacy of chemotherapy. Lin's group reported an intelligent CO nanogenerator CO_2-g-C_3N_4-Au@ZIF-8@F127 (CCAZF) with the ability to trigger the transition from CO_2 to CO and inducing immunogenic cell death (ICD) (Fig. 6D).[116] The reduction from CO_2 to CO was achieved using the g-C_3N_4-Au nanocomposite under 650 nm laser irradiation. After confirming that CO could stimulate a robust immune response, they combined CCAZF with anti PD-L1 (αPD-L1) to inhibit tumor proliferation and metastasis.

Ultrasonic catalysis represents another major conversion method from CO_2 to CO. Li's group used a copper sulfide (CuS) nanosheet as an ultrasound-triggered catalytic nanomaterial and functionalized it with $PMHC_{18}$-PEG_{2000} to improve its biocompatibility (Fig. 6E).[117] The cavitation bubbles formed under ultrasound collapsed and a huge amount of heat and pressure accumulated on the surface of nanomaterials, which provided energy for electrons to be excited to the Fermi level. Then the metastable electrons could be further excited to the B_1 level and CO_2 was reduced to CO owing to the energy matching with the reduction potential of CO_2 to CO (−0.53 V). Similarly, Lin's group constructed BiOBr@Bi_2S_3 nanoheterojunctions to catalyze the formation of CO and hydroxyl radicals (˙OH) under ultrasound irradiation for combined CO therapy and SDT.[118] An MIL-101(Cr)@CoOx nanoplatform fabricated by Li's group also exhibited excellent CO generation ability due to the appropriate band structure and conduction band position.[119]

Unlike O_2 delivery, CO generation strategies must emphasize the safety and targeting precision of CO donors, so more intelligent targeting methods must be involved. Besides, there is still a long way to go before clinical use of CO treatment. To achieve this goal, a more comprehensive understanding of the balance between cytoprotective and cytotoxic effects of CO is essential.

4. NO-mediated cancer therapy

NO is an important gaseous signaling molecule that plays a significant role in the nervous system, cardio-cerebrovascular system, and immune system.[25,120–123] Endogenous NO is produced in the cytoplasm matrix through the oxidation of L-arginine (L-Arg) catalyzed by nitric oxide synthases (NOSs). There are three kinds of natural NOSs in humans, including endothelial nitric oxide synthase (eNOS) distributed in vascular endothelial cells, neuronal nitric oxide synthase (nNOS) distributed in neuron cells, and inducible nitric oxide synthase (iNOS) distributed in immune cells such as lymphocytes and T cells.[120,122,124]

More and more research indicated that NO is a "double-edged sword" in NO-mediated gas therapies.[125,126] Tumor cells keep the intracellular NO level in a safe region, which promotes their survival and growth. Extremely low levels of NO can inhibit tumor progress and metastasis, whereas high concentrations of NO are cytotoxic and can increase their sensitivity to other treatments.

There are mainly five aspects to explain the toxicity of high levels of NO in cancer cells: (1) damaging the mitochondria and

endoplasmic reticulum; (2) reacting with ROS and being converted to more toxic RNS (*e.g.*, $ONOO^-$); (3) causing DNA damage and preventing DNA repair; (4) reversing MDR, especially effective in combination with chemotherapy; (5) inducing immune response and promoting immunotherapy.[125–127]

To accomplish NO-mediated cancer therapy, many strategies are based on targeted NO delivery. Various NO donors have been designed and applied in NO-mediated cancer therapy using nanocarriers. These strategies can be classified into two categories: those activated by endogenous stimuli and those activated by exogenous stimuli.

4.1 NO delivery strategies based on endogenous stimuli

Endogenous stimuli, including pH, GSH, ROS, enzymes and other substances which can stimulate NO production in tumor cells, have been widely applied in NO delivery strategies.

As the natural substrate of NO, L-Arg has been involved in many delivery systems owing to its safety and effectiveness. L-Arg is sensitive to ROS, especially H_2O_2. To increase the rate of catalytic production of NO, ROS providers are often involved in these delivery systems together. For example, Liu's group synthesized porous covalent organic frameworks (COFs) as nanodrug loading platforms to load GOx and L-Arg.[128] At the tumor site, glucose was consumed and decomposed to produce H_2O_2. The abundant endogenous H_2O_2 further reacted with L-Arg to produce a large amount of NO, inducing the lysosomal damage and apoptosis of cancer cells. Chen's group combined GOx-mimicking AuNPs and urchin-like mesoporous organosilica nanoparticles conjugated with L-Arg (UMONs–LA–Au) to enhance cellular uptake and TME-responsive synergistic NO therapy.[129] L-Arg could not be converted to NO owing to the encapsulation of AuNPs and the combination with UMONs through hydrogen bonding and physical adsorption. Only after the cleavage of coordinate bonds at a low pH could AuNPs escape from nanoparticles and catalyze H_2O_2 production. Then, L-Arg was able to react with H_2O_2 and release NO. Recently, Dong's group chose lactate oxidase (Lox) to elevate the cellular H_2O_2 concentration and assist the generation of NO (Fig. 7A).[130] Here, Lox and L-Arg were co-encapsulated into pH-responsive liposomes and then coated with a layer of a homologous cancer cell membrane to generate biomimetic MP@AL nanoparticles. After entering Hepa 1–6 cells, Lox transformed lactic acid, O_2 and H_2O into H_2O_2, which greatly promoted the conversion from L-Arg to NO. In an alternative approach, Zhao's

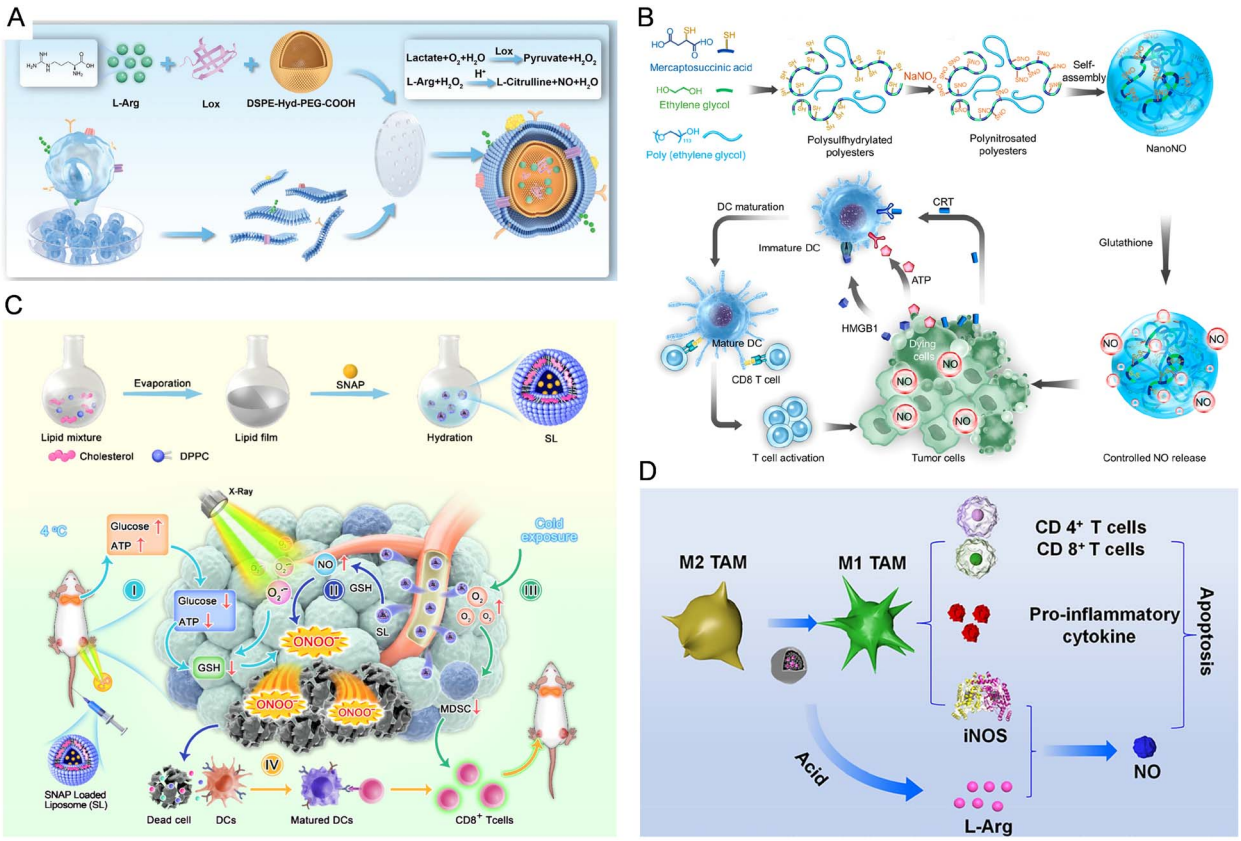

Fig. 7 Endogenous stimuli-triggered NO delivery strategies. (A) The structure of biomimetic MP@AL nanoparticles and the principle of generating H_2O_2 and NO. Reproduced with permission from ref. 130. Copyright 2025 Wiley-VCH GmbH. (B) The synthesis process of a NO nanogenerator and its role in inducing ICD of cancer cells and assisting immunotherapy. Reproduced with permission from ref. 132. Copyright 2022 American Chemical Society. (C) Schematic illustration of the preparation process of the SL nanodrug and the synergistic therapy process in tumor cells. Reproduced with permission from ref. 133. Copyright 2024 American Chemical Society. (D) Schematic illustration of $_{LP}Fe_3O_4$ NPs for pH-responsive gaseous immunotherapy. The M1 TAMs could trigger antitumor responses and convert L-Arg to NO for combating cancer. Reproduced with permission from ref. 136. Copyright 2021 American Chemical Society.

group polymerized L-Arg to form poly L-arginine (PArg) for improving its storage stability and controlling the release of NO.[131] Then, a new kind of nanoparticle (P-lapa-Fc) was fabricated, consisting of hydrophilic PArg, hydrophobic poly(ε-caprolactone) loaded with β-lapachone and ferrocene (Fc), and a pH-sensitive charge-reversal diblock copolymer (PEG-*b*-PDMA). β-Lapachone released in cancer cells could produce a large amount of H_2O_2. H_2O_2 was catalyzed by Fc to produce $^{\bullet}OH$ and $O_2^{\bullet-}$, and NO would further react with $O_2^{\bullet-}$ to yield more toxic $ONOO^-$, which exhibited stronger inhibitory effects on tumors than NO.

GSH can also work as a stimulus for NO generation and has been reported to react with S-nitrosothiol (SNO) groups, *S*-nitroso-*N*-acetylpenicillamine (SNAP), α-(nitrate ester) acetic acid (NEAA), benzofuroxan (BFX) and other compounds. In the work of Wang's group, a well-designed polynitrosated polyester-based NO nanogenerator (NanoNO) showed specific response to thiol-containing molecules such as GSH (Fig. 7B).[132] In the presence of GSH, the homolytic S–N bond in the SNO group was cleaved, releasing enough NO to kill cancer cells. They revealed that NO could induce ICD, which might be due to the increased endoplasmic reticulum stress and mitochondrial dysfunction. NO-treated dying cells acted as vaccines to stimulate the proliferation and activation of T cells. Therefore, the NO nanogenerator was combined with αPD-1 for gas-assisted immunotherapy, which stimulated a systemic immune response of mice and showed satisfactory anti-metastasis ability. Ning's group designed a liposome to load SNAP as a nanodrug to improve the effect of RT and cold exposure therapy (Fig. 7C).[133] Cold exposure therapy was able to relieve tumor hypoxia and cooperate with RT to generate more $O_2^{\bullet-}$. SNAP was sensitive to GSH at the tumor site to release NO. During the RT process, a large amount of $O_2^{\bullet-}$ reacted with NO to form $ONOO^-$ and induce cell death. Yu's group produced an injectable hydrogel (Lapa/CuCys@NO-Gel) based on the H_2O_2 donor β-lapachone, the NO donor NEAA and copper-amino acid mercaptide (CuCys) NPs for tumor therapy.[134] With the joint effort of ROS and RNS, the synthesized Lapa/CuCys@NO-Gel showed a significant suppression effect on tumor growth. In addition, our group developed a COF-based, GSH-triggered NO therapeutic nanoplatform. BFX was loaded into COF NPs to act as an NO provider and HA was coated on the surface of COF to endow the nanoplatform with tumor-targeting capability.[135] Experimental results indicated that 200 μM of GSH in blood and normal cells caused negligible NO generation while 10 mM of GSH in cancer cells led to significantly elevated NO content. It was noteworthy that PDT combined gas treatment produced a "1 + 1 > 2" cancer therapy effect.

Apart from ROS and GSH, pH-stimulated NO precursors have been applied in NO-mediated cancer therapy. For instance, Zhang's group constructed poly(acrylic acid) (PAA) wrapped hollow Fe_3O_4 NPs to encapsulate L-Arg ($_{LP}Fe_3O_4$) for pH-responsive gaseous immunotherapy (Fig. 7D).[136] In acidic tumor microenvironments, the polymer shell of $_{LP}Fe_3O_4$ NPs gradually loosened and released L-Arg due to electrostatic repulsion. Meanwhile, under the stimulation of Fe_3O_4 NPs, immunosuppressive M2 TAMs were reprogrammed to the immunostimulatory M1 phenotype, resulting in the release of pro-inflammatory cytokines and the recruitment and activation of $CD4^+$ and $CD8^+$ T cells. Compared to M2 TAMs, iNOS was overexpressed in M1 TAMs, which effectively catalyzed L-Arg to generate NO. Yang's group entrapped the NO prodrug O_2-(2,4-dinitrophenyl) 1-[(4-ethoxycarbonyl) piperazin-1-yl] diazen-1-ium-1,2-diolate (JS-K) in liposomes modified with sphingosine-1-phosphate (S1P)-signaling targeting molecules for glioblastoma multiforme inhibition, which could react with overexpressed glutathione S-transferase to generate NO with the joint action of GSH and H^+.[137] S1P specifically conjugated with S1P receptors to downregulate P-gP expression and helped more S1P/JS-K/Lipo to accumulate in the glioma region and penetrate the blood–brain–tumor barrier. Compared with non-targeting JS-K/Lipo, S1P/JS-K/Lipo exhibited more efficient cellular internalization and a higher NO level in U87MG cells. In addition, NO may regulate angiogenesis and normalize tumor vessels. Therefore, Chen's group designed stable NO-releasing agents (NanoNO) with $[Fe(\mu\text{-}SEt)_2(NO)_4]$ (DNIC) as an NO donor.[138] NanoNO exhibited pH-dependent NO release characteristic and a dose-dependent anti-cancer effect. Besides, they investigated the influence of NO on the tumor and peripheral blood vessels. Both *in vitro* and *in vivo* results suggested that low doses of NO could normalize tumor vessels, enhance drug penetration, shift an immunosuppressive TME to an immunostimulatory TME, and suppress tumor metastasis.

4.2 NO delivery strategies based on exogenous stimuli

In addition to the endogenous stimulation methods mentioned above, exogenous stimulation methods also contributed to the delivery of NO, such as light, ultrasound, X-rays and heat.

Some NO release strategies based on exogenous light irradiation have been established. For example, Zhang's group chose a NO-conjugated cationic lipid (DPNO(Zn)) as an NO donor and Ce6 as a photosensitizer to form lipid nanoparticles (CNOs).[139] In order to improve biocompatibility, CNOs were further coated with γPGA to form PCNOs. Under ultraviolet (UV) light or 660 nm laser irradiation, PCNOs could release NO or $^1O_2$ rapidly and these reactive species caused cell death through multiple pathways. Yang's group developed a carbon-dots-doped g-C_3N_4 nanomaterial modified with poly-L-arginine (ArgCCN).[140] Under red light excitation, ArgCCN generated H_2O_2 *via* water oxidation mediated by photogenerated holes and further oxidized L-Arg to generate NO. Unlike traditional mechanisms, they selected hole-mediated oxidation of the NO donor, so the hypoxic microenvironment blocked ROS generation largely but had little impact on NO-mediated cancer inhibition. Besides, He's group designed an oligoarginine domain (RRR) as a NO donor and combined it with Ce6 for light-triggered ROS generation.[141] ROS reacted with RRR to release NO and further yielded toxic $ONOO^-$ to induce cell apoptosis.

Light-emitting diodes (LEDs) have become a novel light source in phototherapy. Zhang's group reported an implantable NO-release device based on a wirelessly powered LED (wLED) and a NO donor *S*-nitrosoglutathione (GSNO).[142] The wLED device could be lit up using a wireless charging device and give

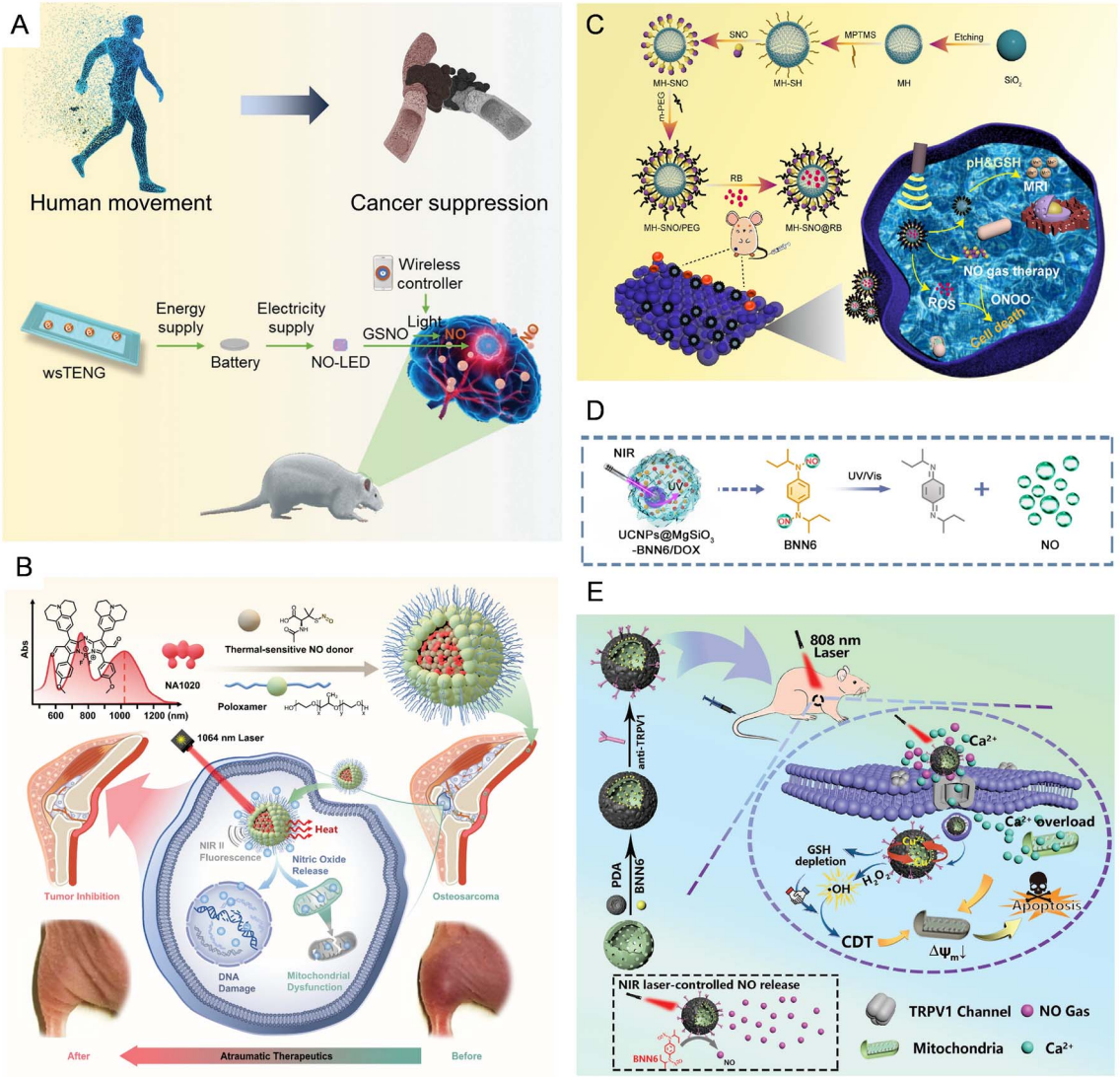

Fig. 8 Exogenous stimuli-triggered NO delivery strategies. (A) Schematic illustration of a self-powered wireless system for intracranial neuroglioma therapy. Reproduced with permission from ref. 143. Copyright 2022 Wiley-VCH GmbH. (B) The chemical structure of NA1020 and the components of NA1020-NO@PLX. Under laser irradiation, NO was released during the PTT process performed using NA1020-NO@PLX. Reproduced with permission from ref. 146. Copyright 2023 Wiley-VCH GmbH. (C) Schematic illustration of the preparation process of MH-SNO@RB nanoparticles and ultrasound-triggered SDT and NO-mediated gas therapy. Reproduced with permission from ref. 148. Copyright 2023 American Chemical Society. (D) Schematic illustration of UCNPs@$MgSiO_3$-BNN6/DOX NPs for UV/Vis-triggered BNN6 activation. Reproduced with permission from ref. 149. Copyright 2020 American Chemical Society. (E) The preparation process of an HCuS@PDA-TRPV1/BNN6 nanoplatform and its mechanism of action in tumor cells. Reproduced with permission from ref. 150. Copyright 2024 Wiley-VCH GmbH.

out light of different wavelengths. Then, GSNO was able to release NO under light irradiation. Under the remote control of a mobile phone, the wLED could switch "on" or "off" on demand for controlled NO generation. This NO-wLED device provided a promising future for remote controlled NO therapy. Besides, Li's group fabricated an integrated and self-powered wireless system for neuroglioma gas therapy (Fig. 8A).[143] Firstly, they made stretchable single-electrode mode triboelectric nanogenerators (wsTENGs), which could be attached to skin and collect and transfer mechanical energy from body movements to electricity. Secondly, NO-LED, a NO-releasing device composed of a blue light LED and GSNO, was implanted in the brain of mice. Finally, the NO-LED was controlled using a smartphone wirelessly for controlled light stimulation and NO release. *In vitro* and *in vivo* experimental results all illustrated the outstanding performance of controlled NO generation for intracranial neuroglioma using the NO-LED + wsTENG.

Some researchers are aiming to take advantage of heat in cellular NO delivery, and photothermal conversion is an ideal approach to achieve this. Based on this foundation, SNO conjugated Mn-porphyrin NMOFs were constructed by Yin's group for combined magnetic resonance (MR) imaging, NO-mediated gas therapy and PTT.[144] Similarly, Chen's group used polydopamine (PDA) as the photothermal conversion agent to stimulate the release of NO from SNO.[145] Heat caused by MOFs or PDA elevated local temperature, which not only

achieved PTT, but also cut off the S–N bond in SNO to release NO for gas therapy. Besides, Huang's group encapsulated the organic photothermal agent aza-BODIPY (NA1020) and the heat-sensitive NO donor (SNAP) into an amphiphilic polymer (PLX) to develop a gas/phototheranostic nanocomposite (NA1020-NO@PLX), which could be used for low-temperature PTT and photothermal-triggered NO therapy under 1064 nm laser irradiation (Fig. 8B).[146]

Besides, ultrasound-irradiated NO generation has been employed in NO-mediated cancer therapy. Some strategies are based on ROS generated under ultrasound irradiation and the subsequent release of NO caused by ROS. For example, Lin's group reported a synergistic sonodynamic/gas therapy nanovaccine based on L-Arg-loaded black mesoporous titania and αPD-L1 (BMT@LA NCs).[147] This nanoplatform possessed the abilities of ultrasound-triggered $^1O_2$ production and NO release. Under ultrasound irradiation, BMT@LA NCs could not only stimulate BMT to produce $^1O_2$, but also oxidize L-Arg to produce NO. Furthermore, $^1O_2$ in turn promoted the generation of NO. Other strategies are based on the structural changes of NO donors directly caused by ultrasound irradiation, such as the breakage of chemical bonds. For instance, SNO groups could release NO through exogenous stimuli to break the S–NO chemical bonds with lower bond energy. Wu's group attached SNO groups to the surface of manganese-doped hollow mesoporous silica nanoparticles and then loaded the sonosensitizer Rose Bengal (RB) inside it to fabricate MH-SNO@RB nanoparticles (Fig. 8C).[148] The MH-SNO@RB nanoparticles were able to release ROS and NO under ultrasound stimulation, which could react with each other to generate $ONOO^-$ for efficient cancer therapy.

N,*N*′-di-*sec*-butyl-*N*,*N*′-dinitroso-1,4-phenylenediamine (BNN6) is a small organic molecule NO donor that can be activated using light or ultrasound to release NO. For example, Yang's group designed an upconversion nanosystem for NIR-triggered NO delivery and MDR reversal. UCNPs upconverted NIR light to UV/vis light, which in turn activated BNN6 (Fig. 8D).[149] NO generated in cancer cells inhibited ubiquitin–proteasome and down-regulated the NF-κB signaling pathway, thus preventing drug efflux and reversing drug resistance. Besides, Li's group (Fig. 8E) developed a NIR-triggered NO-releasing nanoplatform (HCuS@PDA-TRPV1/BNN6) consisting of PDA-coated hollow CuS nanoparticles and BNN6.[150] The PDA layer was able to convert the photons into active electrons and induce NO release from BNN6. In addition to light, ultrasound was also applied in BNN6-mediated NO release. In the research of Yang's group, BNN6 and Gd^{3+}-coordinated Ce6 were conjugated to oxidized g-C_3N_4 NSs for MRI-guided gas therapy and SDT.[151] Under ultrasound irradiation, ROS and NO were produced simultaneously, inducing mitochondrial damage, DNA damage and cancer cell death.

As a star molecule, NO has provided us with countless promising ideas for gas-mediated cancer treatment. In the past several decades, research on its mode of intracellular production and mechanism of action has been extensive. However, there are still many problems to be solved before clinical trials, including a more comprehensive understanding of NO's double-edged nature, easier and less toxic synthesis of NO donors and prevention of premature NO leakage.

5. H_2-mediated cancer therapy

H_2, the gas with the smallest molecular weight, can penetrate the cell membrane easily and diffuse to various organelles freely. In 1975, the first research on H_2-mediated therapy of squamous cell carcinoma was reported.[152] Since then, as a new type of therapeutic gas, H_2 began to gain attention. According to existing research, H_2 has anti-oxidation and anti-inflammatory capacities, which make it a promising direction for the development of gas-mediated cancer therapy.[28,153]

Compared with other therapeutic gases, the anti-tumor mechanism of H_2 is less clear, but some possible cellular regulation approaches related to H_2-mediated gas therapy have been explored. Firstly, H_2 can serve as an antioxidant by scavenging free radicals selectively (*e.g.*, $^{\bullet}OH$ and $ONOO^-$). However, this process may destroy redox homeostasis and induce ROS rebound quickly and violently, which finally results in overproduced ROS and more severe oxidative stress.[154,155] Secondly, ATP generation will be blocked once H_2 diffuses to mitochondria and then the expression of P-gP is suppressed. On this basis, many drug delivery strategies have been combined with H_2 generation to achieve higher delivery efficiencies.[156]

There are two main methods of H_2 generation: *in situ* reactions and direct transportation. *In situ* reactions include the reduction of protons and the electrolysis of water, and direct transportation is mainly based on delivery nanosystems.

5.1 H_2 release based on exogenous stimuli

Various exogenous stimuli, including light, ultrasound and X-rays, are involved in H_2 generation strategies.

Light irradiation can be used to control the release of H_2 based on some inorganic nanoplatforms. For example, He's group reported a novel drug-free therapeutic strategy for combined hole/gas therapy by employing Z-scheme $SnS_{1.68}$–$WO_{2.41}$ as a photocatalyst (Fig. 9A).[157] Under NIR irradiation, electron–hole pairs were separated on the surface of $SnS_{1.68}$–$WO_{2.41}$. Then GSH was oxidized by the holes on $WO_{2.41}$ nanodots while H^+ was reduced by the electrons to generate H_2 on $SnS_{1.68}$ nanoplates. DNA damage caused by overproduction of H_2 led to irreversible damage and death of tumor cells. This drug-free therapy strategy showed an effective tumor suppressive ability. Similarly, [FeFe]-hydrogenase ([FeFe]-TPP) and carbon/potassium-doped red polymeric carbon nitride (RPCN) have also been selected as H_2 producers for *in situ* H_2 generation under laser irradiation.[156,158]

In addition, some anaerobic photosynthetic bacteria with H_2 production abilities were used to design light-activated H_2 generators. For example, Cai's group designed small-sized gold nanoparticle (Au NP) engineered *Rhodospirillum rubrum* (R.r-Au) to deplete lactate and generate H_2.[159] Au NPs were able to absorb light and convert it into electrons, which were transferred to *Rhodospirillum rubrum* to accelerate the production of H_2 catalyzed by nitrogenase. Recently, Gao's group used *Rhodobacter*

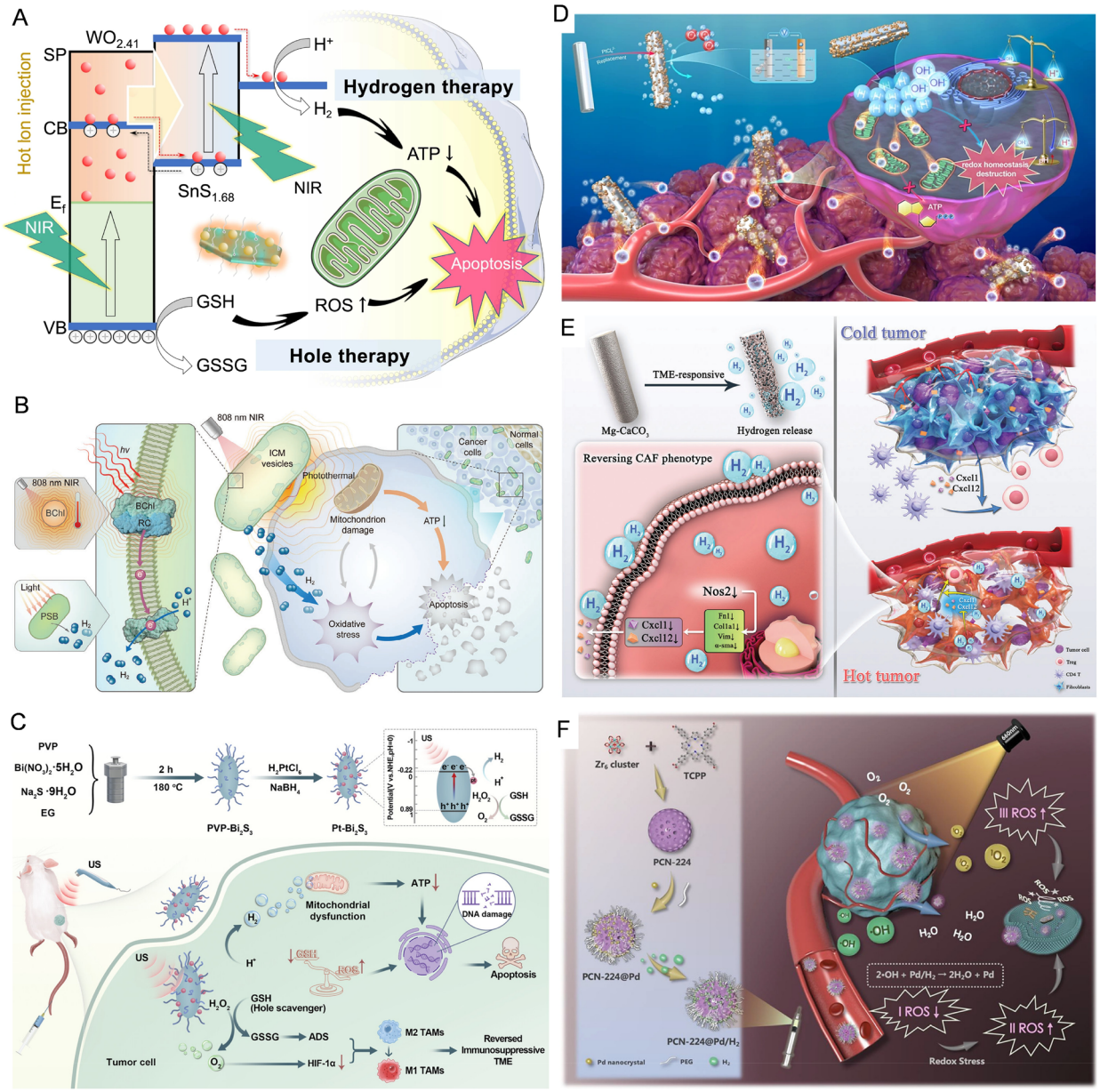

Fig. 9 H_2-mediated gas therapy strategies. (A) Schematic illustration of the hole/H_2 therapy strategy with a Z-scheme $SnS_{1.68}$–$WO_{2.41}$ nanocatalyst. Reproduced with permission from ref. 157. Copyright 2021 Springer Nature. (B) The hydrogen production and photothermal conversion processes of *R. sphaeroides*. Reproduced with permission from ref. 160. Copyright 2025 Wiley-VCH GmbH (C) Schematic illustration of the preparation process of Pt–Bi_2S_3 and its ability to generate H_2 and O_2 for cell apoptosis and immunosuppressive TME reversal. Reproduced with permission from ref. 162. Copyright 2023 Wiley-VCH GmbH. (D) The H_2 generation process of MgG rods and their role in cancer therapy. Reproduced with permission from ref. 165. Copyright 2022 Springer Nature. (E) Schematic illustration of acidic TME-responsive Mg–$CaCO_3$ nanorods in H_2 generation and tumor remodeling. Reproduced with permission from ref. 166. Copyright 2024 Wiley-VCH GmbH. (F) The synthesis process of a PCN-224@Pd/H_2 nanosystem and the principle of oxidative stress induced by it. Reproduced with permission from ref. 155. Copyright 2020 Wiley-VCH GmbH.

sphaeroides (*R. sphaeroides*) to absorb an 808 nm laser for long-term H_2 production and photothermal conversion (Fig. 9B).[160] High concentrations of H_2 induced oxidative stress and elevated temperature disrupted mitochondrial function, which ultimately led to cancer cell apoptosis.

Yang's group constructed an X-ray triggered H_2 generator (Au–TiO_2@ZnS) for synergistic gas-/radio-therapy.[161] Dumbbell-shaped Au–TiO_2 heterojunction structures were synthesized and combined with long afterglow materials. The H_2 generation capacity of the nanoparticles included two aspects: one was the reduction of H_2O to H_2 on the surface of Au under direct X-ray irradiation; the other was the reduction reaction that happened on the surface of TiO_2 due to electrons escaping from afterglow emission. In general, the effective H_2 generator improved the therapeutic effect and reduced the side effects of X-rays owing to the anti-inflammatory characteristic of H_2.

Table 1 Generation/delivery methods, therapeutic mechanisms, advantages and disadvantages of gas-mediated cancer therapy

Gas	Generation/delivery methods	Therapeutic mechanisms	Advantages	Disadvantages	Ref.
O_2	• Delivery systems based on O_2 carriers	• Relieving tumor hypoxia	• Improving the foundation of the TME	• Poor tumor targeting ability	52–54, 61, 62, and 68–70
	• Decomposing H_2O_2 to produce O_2	• Inhibiting the activity of HIF-1α			
	• Generating O_2 through *in situ* reactions	• Preventing chemotherapy-induced tumor resistance • Providing raw materials for ROS generation	• Good synergistic effect with various therapies	• Difficult to achieve long-term and continuous O_2 supply	
	• Reducing O_2 consumption within tumor cells	• Enhancing the efficacy of RT, PDT, *etc.*	• Diverse generation and delivery methods	• Poor temporal and spatial controllability	
CO	• Releasing CO from metal-carbonyl complexes under stimulations	• Blocking mitochondrial electron transport chain and ATP supply	• Strong ability to kill tumor cells	• May lead to CO poisoning	82, 86–91, 103–105, and 114–116
		• Intensifying oxidative stress	• Good temporal and spatial controllability		
	• Releasing CO from metal-free CORMs	• Inhibiting tumor metastasis			
	• The transformation from CO_2 to CO	• Enhancing the EPR effect and promoting drug accumulation	• Effective for multiple types of tumors	• Narrow therapeutic concentration range	
NO	• Releasing NO in response to pH, GSH, ROS, enzymes and other endogenous stimuli	• The generation of highly toxic RNS • Inhibiting mitochondrial respiration	• Diverse intracellular action pathways	• Difficulties in achieving precise dosage control	131–134, 149, and 151
		• Causing DNA damage	• Concentration-dependent versatility	• Short half-life of NO	
	• Releasing NO in response to light, heat, ultrasound and other exogenous stimuli	• Inducing immune response • Reversal of chemotherapy resistance	• Precise targeted delivery and controlled release	• May lead to systemic side effects	
H_2	• Releasing H_2 in response to H^+, GSH, ROS, enzymes and other endogenous stimuli	• Anti-oxidation and anti-inflammatory	• Protecting normal cells	• High diffusibility and poor retention at the tumor site	154–157, 161, and 166
	• Releasing H_2 in response to light, ultrasound, electricity and other exogenous stimuli	• The rebound of ROS		• Limited anti-cancer effect	
		• Downregulation of P-gp			
	• Using H_2 storage materials	• Causing DNA and mitochondrial damage	• High biological safety	• Unclear therapeutic mechanism	

Ultrasound-excited H_2 generation has also been explored. Lin's group reported an ultrasound-excited H_2 and O_2 generation strategy based on metal–semiconductor heterostructure nanocomposites for hypoxia reversal and H_2 therapy (Pt–Bi_2S_3) (Fig. 9C).[162] Hole–electron separation occurred under ultrasound irradiation. Owing to the more negative conduction band edge than the redox potential of H^+/H_2, Bi_2S_3 and Pt–Bi_2S_3 could catalyze the reduction of H^+/H_2O to H_2 easily. Meanwhile, the holes with high oxidation ability could oxidize GSH to GSSG, prevent the recombination of electrons and holes, and maintain long-term H_2 generation. In addition, the holes also reacted with H_2O_2 to produce O_2 for hypoxia relief. The conversion of M2 macrophages to M1 macrophages proved the reversal of the immunosuppressive TME. As an effective H_2 and O_2 generator, Pt–Bi_2S_3 achieved a synergistic tumor-killing ability.

In addition, some papers involved electrochemistry in intracellular H_2 generation. Jin's group innovatively used traditional Chinese acupuncture iron needles as electrodes to develop a H_2 generation system (H_2-ECT) for selective H_2 therapy in an acidic tumor microenvironment.[163] The acupuncture electrodes were punctured into the acidic tumor area, and the H_2 evolution reaction occurred on the cathode. Later, they upgraded this system (H_2-EC/SD) to realize the "domino effect" for tumor elimination and postoperative anti-inflammation.[164] Under ultrasound irradiation, H_2 ablated tumors by causing a temperature increase through bubble cavitation and inhibiting mitochondrial respiration. Fe^{2+} generated in the anode also played a certain role in tumor inhibition by promoting the production of ROS. Besides, Cheng's group implanted a Mg-based galvanic cell (MgG) into tumors for H_2-mediated cancer therapy (Fig. 9D).[165] Compared with bare Mg rods, the much lower corrosion potential of MgG rods enabled them to produce H_2 more rapidly and more violently. Besides, the residual product $Mg(OH)_2$ would neutralize the acidic environment, which helped improve the killing ability of CD8+ T cells.

5.2 H_2 release based on endogenous stimuli

At present, H_2 release triggered by endogenous stimulation is mainly achieved through the response to the acidic microenvironment of the tumor. Fu's group designed $CaCO_3$ nanoparticle-coated magnesium rods (Mg–$CaCO_3$) for controllable and TME-responsive H_2 release (Fig. 9E).[166] $CaCO_3$ was decomposed in the acidic microenvironment, so Mg could react with H^+ to produce a large amount of H_2. Experimental results showed that H_2 therapy could not only induce severe mitochondrial damage in cancer cells, but also reduce intracellular ROS levels in cancer-associated fibroblasts (CAFs). This strategy downregulated the expression of NOSs in CAFs, reversed the tumor-promoting and immunosuppressive phenotypes of CAFs, and thereby improved the immune response.

Besides, ammonia borane (AB) has been widely used as a H_2 donor due to its ability to react with H^+/H_2O in the acidic TME to release H_2. Melanoma cancer stem cells (CSCs) are closely related to the pathogenesis, development, metastasis and recurrence of melanoma. But the immune evasion of CSCs is a major obstacle to melanoma treatment. To solve this problem, AB-loaded nanoparticles combined with a wearable silk-based microneedle device (SMND) were developed by Xie's group.[167] Thermally responsive polycaprolactone (PCL) was coated on the surface of AB-loaded mesoporous silica nanoparticles (AB-MSNs). The microneedle was embedded into the tumor site and heated up to 50 °C. Then the PCL changed from solid to liquid, thus enabling the release of AB-MSNs. In the acidic TME, AB reacted with H^+ to generate H_2, which could consume ROS, inhibit tumor cell proliferation and disrupt CSC heterogeneity.

5.3 Direct transportation of H_2

In addition to designing H_2 generation strategies, some researchers tried to use H_2 storage materials for intracellular H_2 delivery. Pd has a strong affinity for H_2 and is often utilized as a "warehouse" for H_2 storage. Consequently, many novel H_2 delivery nanosystems have been developed based on Pd atoms and their derivatives.

For instance, He's group synthesized cubic Pd nanocrystals as a H_2 host to deliver H_2 *via* the EPR effect.[154] After hydrogenation, $PdH_{0.2}$ nanocrystals exhibited stronger VIS–NIR-zone absorption than Pd, which was beneficial for photoacoustic imaging and PTT. Notably, the intracellular ROS levels of cells treated with $PdH_{0.2}$ all rose first and then fell. The increase in ROS levels was on account of the stress response to $PdH_{0.2}$, while the decrease in ROS levels was because H_2 released from $PdH_{0.2}$ had the ability to eliminate ROS. Lower ROS levels in normal cells could be returned to the normal level and harmful side effects could be avoided. However, the overhigh ROS level in cancer cells could not return to the normal level and induced oxidative stress. Combined with PTT under NIR irradiation, $PdH_{0.2}$ ultimately caused cell apoptosis and tumor inhibition. Zhu's group proposed a Pd-engineered MOF (denoted as PCN-224@Pd/H_2) for H_2 delivery and synergistic gas/photodynamic therapy (Fig. 9F).[155] According to experimental results, PCN-224@Pd/H_2 possessed both long lasting H_2 release ability and $^1O_2$ generation properties without mutual interference. Both studies confirmed a common phenomenon in cancer cells: compared with normal cells, tumor cells had higher ROS levels and were more sensitive to reductive H_2, so they exhibited a lower ROS loss percentage but much higher rebound. Ultimately, overproduced ROS caused severe oxidative stress and cell apoptosis.

H_2-mediated gas therapy is still in its infancy, but existing research has indicated that it is a promising direction in the near future. Next, researchers should focus on the mechanism of H_2-mediated therapies in cells. At the same time, more precise H_2 delivery methods and materials should be developed and applied.

6. Conclusions and perspectives

Significant advances and innovative breakthroughs have been made in gas-mediated anti-tumor therapy. Various therapeutic strategies based on O_2, CO, NO and H_2 have been designed and applied in experimental research. In these studies, organic/

inorganic donors with rational chemical modifications have demonstrated improved gas production performance. A wide range of nanocarriers have been used for active/passive tumor-targeted delivery, such as polymers, Au NPs, MOFs, COFs and liposomes.[137,168–185] Furthermore, researchers have increasingly integrated gas therapy with other therapeutic modalities and imaging techniques, significantly improving their anti-tumor performance and imaging capabilities. Nevertheless, several key challenges remain to be addressed.

First, a more comprehensive and deeper understanding of the anti-tumor effects of therapeutic gases is essential. Current research on the mechanisms of gas-based cancer therapy remains insufficient, especially for H_2. Compared with other gases, H_2-mediated therapies are relatively underexplored. The anti-tumor mechanism of H_2 mainly involves anti-oxidative stress, but its target network has not yet been systematically established. In addition, the action pathways of gas molecules have not been fully analyzed. For example, while CO has been shown to inhibit heat shock proteins and enhance PTT, the precise signaling pathways involved are still unclear. Furthermore, studies have shown that most gases can cause changes in cellular functions, especially in the mitochondria, endoplasmic reticulum and nucleus. However, studies on the changes in other cellular organelles are relatively scarce. This is also one of the key aspects that require further exploration. Apart from organelles, the biological processes of cells also depend on various microenvironments, such as pH, viscosity, polarity, *etc.* These changes not only alter the life activities of cells but also affect the treatment process. For instance, an acidic environment is more conducive to the generation of $^{\bullet}OH$, while a relatively basic environment is more favorable for the formation of $O_2^{\bullet-}$.[186–189] During the treatment process, fluctuations in pH may cause alterations in the production of key active substances, thereby resulting in different therapeutic outcomes. Such changes require further in-depth research and applications.

Second, precise control of gas dosage remains challenging, and real-time monitoring methods are critically lacking. The therapeutic effect of gases on tumor progression is highly concentration-dependent. However, it is difficult to monitor the kinetics of gas release *in vivo*, which may lead to ineffectiveness or toxic side effects. Therefore, future gas donors should not only achieve gas delivery or generation but also enable precise control over release kinetics, temporal regulation, and termination capability to ensure on-demand gas therapy.

Third, improving targeting specificity remains critical. On the one hand, distinguishing cancer cells from normal cells is a key factor to be considered in the design of gas donors. Despite their favorable diffusion properties, gas molecules still exhibit significant off-target distribution. Therefore, more comprehensive, multi-level targeting systems need to be designed. A promising approach involves combining tumor-targeting ligands with endogenous and exogenous stimulus-responsive groups. On the other hand, more effective targeting strategies could be developed by focusing on the primary sites of gas activity. For example, since CO is more inclined to inhibit mitochondrial respiration, dual-targeting strategies that integrate cancer cell and mitochondrial targeting groups may enable precise gas delivery to key subcellular regions, thereby enhancing therapeutic outcomes.

Fourth, simplifying system design and the biosafety of nanomaterials are also critical considerations. While multi-functional gas delivery systems can provide enhanced capabilities, complex designs may increase the risk of unpredictable toxicity. To solve this problem, the design of nanomaterials should be reasonably simplified, and the use of materials with unclear biocompatibility should also be minimized. In addition, the stability of gas delivery nanosystems is an indispensable factor. For instance, liposomes with excellent biocompatibilities have been extensively used in drug delivery, but their instability often leads to premature drug leakage during blood circulation. Therefore, new nanocarriers with simplified synthesis and better biocompatibility are expected to be discovered. Besides, more rigorous preclinical evaluation is necessary, including tests of stability, biodistribution, and metabolism.

Finally, the combination of gas therapy and other therapies should be further diversified. To date, the most popular combination mode is gas therapy and phototherapy. In these cases, light serves both as a therapeutic modality and a trigger for gas release. These combinations typically exhibit enhanced therapeutic efficacy compared to single treatments. However, integrations of gas therapy with SDT, chemotherapy, immunotherapy and gene silencing therapy are relatively rare. Besides, the development of nanoplatforms capable of delivering multiple therapeutic gases simultaneously is still in its early stage. The synergistic effects among therapeutic gases are highly promising. These areas represent important avenues for future investigation.

This review systematically summarized and compared the unique mechanisms of action and application prospects of four gas molecules (O_2, CO, NO, and H_2) in cancer treatment. It focused on the recent articles in this area and conducted a horizontal comparison of the generation and delivery methods, therapeutic mechanisms, advantages and disadvantages of these gases (Table 1). Moreover, we have introduced how to use these intelligent platforms to achieve targeted delivery, controlled release, and tumor killing of gas molecules. Additionally, we provided some significant and scientifically promising development directions for gas therapy. The cancer gas therapy strategies summarized in this review mostly focus on improving the accuracy of delivery and enhancing drug efficacy. These methods are not only beneficial for reducing drug dosage and minimizing waste, but can also help avoid drug pollution and reduce reliance on drug degradation methods. This represents an important approach to develop more people-oriented and sustainable models of cancer treatment. Despite the considerable accomplishments in gas therapy, there are still many obstacles to be overcome before clinical application. A deeper understanding of the mechanisms, accurate targeting, controllable release, and reduced side effects represents key directions for the future development of gas therapy. We hope that this article can provide an important theoretical basis and directional guidance for the

development of next generation universal, precise and efficient cancer treatment strategies based on gas molecules. We believe that gas therapy has the potential to distinguish itself as an innovative modality in the future of cancer treatment.

Author contributions

J. Y., J. Z., Y. L., N. L. and B. T. conceived the outline of the manuscript. J. Y., J. Z., W. P., Y. L., and N. L. wrote and revised the manuscript.

Conflicts of interest

There are no conflicts to declare.

Data availability

No primary research results, software or code have been included and no new data were generated or analysed as part of this review.

Acknowledgements

This work was supported by the Natural Science Foundation of Shandong Province (Major Basic Research Project, ZR2023ZD44; ZR2024LMB006) and the project of Shandong Provincial Center for Fundamental Science Research (YDZX2024150).

References

1 S. Tohme, R. L. Simmons and A. Tsung, *Cancer Res.*, 2017, **77**, 1548–1552.
2 M. Dankner, M. Caron, T. Al-Saadi, W. Yu, V. Ouellet, R. Ezzeddine, S. M. Maritan, M. G. Annis, P. U. Le, J. Nadaf, N. S. Neubarth, P. Savage, D. Zuo, C. P. Couturier, J. Monlong, H. Djambazian, H. Altoukhi, G. Bourque, J. Ragoussis, R. J. Diaz, M. Park, M.-C. Guiot, S. Lam, K. Petrecca and P. M. Siegel, *Neuro-Oncology*, 2021, **23**, 1470–1480.
3 X. Jin, H. Han and Q. Liang, *Front. Oncol.*, 2024, **14**, 1412367.
4 Z. B. Ejder and N. Sanlier, *Support. Care Cancer*, 2023, **31**, 683.
5 I. I. Verginadis, D. E. Citrin, B. Ky, S. J. Feigenberg, A. G. Georgakilas, C. E. Hill-Kayser, C. Koumenis, A. Maity, J. D. Bradley and A. Lin, *Lancet*, 2025, **405**, 338–352.
6 Brianna and S. H. Lee, *Med. Oncol.*, 2023, **40**, 88.
7 S. Li, Z. Zhang, W.-F. Lai, L. Cui and X. Zhu, *Biomed. Pharmacother.*, 2020, **130**, 110639.
8 M. Lacouture and V. Sibaud, *Am. J. Clin. Dermatol.*, 2018, **19**, 31–39.
9 K. L. A. Chan and P. L. V. Fale, *Anal. Chem.*, 2014, **86**, 11673–11679.
10 R. C. Bensen, S. J. Standke, D. H. Colby, N. R. Kothapalli, A. T. Le-McClain, M. A. Patten, A. Tripathi, J. E. Heinlen, Z. Yang and A. W. G. Burgett, *ACS Pharmacol. Transl. Sci.*, 2021, **4**, 96–100.
11 N. Raeisi-Kheirabadi and A. Nezamzadeh-Ejhieh, *ChemistrySelect*, 2022, **7**, e202203788.
12 S. Koganemaru, T. Kawai, H. Fuchigami, N. Maeda, K. Koyama, Y. Kuboki, T. Mukohara, T. Doi and M. Yasunaga, *Br. J. Pharmacol.*, 2023, **180**, 762–774.
13 N. Pan, S. J. Standke, N. R. Kothapalli, M. Sun, R. C. Bensen, A. W. G. Burgett and Z. Yang, *Anal. Chem.*, 2019, **91**, 9018–9024.
14 N. Raeisi-Kheirabadi, A. Nezamzadeh-Ejhieh and H. Aghaei, *ACS Omega*, 2022, **7**, 31413–31423.
15 Y. Wang, T. Yang and Q. He, *Natl. Sci. Rev.*, 2020, **7**, 1485–1512.
16 R. Liu, Y. Peng, L. Lu, S. Peng, T. Chen and M. Zhan, *J. Nanobiotechnol.*, 2021, **19**, 443.
17 P. Ghaffari-Bohlouli, H. Jafari, O. V. Okoro, H. Alimoradi, L. Nie, G. Jiang, A. Kakkar and A. Shavandi, *Small Methods*, 2024, **8**, 2301349.
18 R. Motterlini and L. E. Otterbein, The therapeutic potential of carbon monoxide, *Nat. Rev. Drug Discovery*, 2010, **9**, 728–743.
19 A. Sahu, I. Kwon and G. Tae, *Biomaterials*, 2020, **228**, 119578.
20 D. Gao, S. Asghar, R. Hu, S. Chen, R. Niu, J. Liu, Z. Chen and Y. Xiao, *Acta Pharm. Sin. B*, 2023, **13**, 1498–1521.
21 S. Li, R. Liao, X. Sheng, X. Luo, X. Zhang, X. Wen, J. Zhou and K. Peng, *Front. Oncol.*, 2019, **9**, 696.
22 L. Jia, Y. Hong, X. He, Y. Zhou, L. Ren, H. Du, B. Zhao, B. Qin, Z. Yang and D. Gao, *Chin. Chem. Lett.*, 2025, **36**, 109957.
23 S. B. Wiegand, L. Traeger, H. K. Nguyen, K. R. Rouillard, A. Fischbach, F. Zadek, F. Ichinose, M. H. Schoenfisch, R. W. Carroll, D. B. Bloch and W. M. Zapol, *Redox Biol.*, 2021, **39**, 101826.
24 H. Zhang, W. Jiang, Y. Peng, J. Yang, X. Chu, Z. Long, R. Li, Q. Liang, H. Suo, S. Wang, M. Yang, J. Qi, D. Ding, Y.-W. Yang and B. Wang, *Biomaterials*, 2022, **286**, 121577.
25 C. Farah, L. Y. M. Michel and J.-L. Balligand, *Nat. Rev. Cardiol.*, 2018, **15**, 292–316.
26 B. Zhou, M. Zulpya, S. Wang, Z. Wang, J. Sun, Y. Cui, L. Sun, L. Xu, H. Liu and B. Dong, *J. Colloid Interface Sci.*, 2025, **694**, 137724.
27 H. Liu, X. Kang, P. Ren, X. Kuang, X. Yang, H. Yang, X. Shen, H. Yan, Y. Kang, F. Zhang, X. Wang, L. Guo and W. Fan, *Int. Immunopharmacol.*, 2023, **120**, 110252.
28 Y. You, J. Jiang, G. Zheng, Z. Chen, Y.-X. Zhu, H. Ma, H. Lin, X. Guo and J. Shi, *Adv. Mater.*, 2024, **36**, 2311429.
29 H. Chen, Y. Guo, Z. Zhang, W. Mao, C. Shen, W. Xiong, Y. Yao, X. Zhao, Y. Hu, Z. Zou and J. Wu, *Nano Lett.*, 2022, **22**, 229–237.
30 Q. Yousefi and A. Nezamzadeh-Ejhieh, *Solid State Sci.*, 2024, **154**, 107584.
31 Q. Yousefi and A. Nezamzadeh-Ejhieh, *Int. J. Biol. Macromol.*, 2024, **283**, 137717.
32 A. Nezamzadeh-Ejhieh and S. Tavakoli-Ghinani, *C. R. Chim.*, 2014, **17**, 49–61.

33 N. Yang, F. Gong and L. Cheng, *Chem. Sci.*, 2022, **13**, 1883–1898.
34 Y.-Z. Jing, S.-J. Li and Z.-J. Sun, *J. Mater. Chem. B*, 2021, **9**, 8541–8557.
35 G. R. Navale, S. Singh and K. Ghosh, *Coord. Chem. Rev.*, 2023, **481**, 215052.
36 C.-C. Huang, W.-T. Chia, M.-F. Chung, K.-J. Lin, C.-W. Hsiao, C. Jin, W.-H. Lim, C.-C. Chen and H.-W. Sung, *J. Am. Chem. Soc.*, 2016, **138**, 5222–5225.
37 Z. Yang and H. Chen, *Nano Res.*, 2023, **16**, 3924–3938.
38 D. Wang, H. Wu, S. Z. F. Phua, G. Yang, W. Qi Lim, L. Gu, C. Qian, H. Wang, Z. Guo, H. Chen and Y. Zhao, *Nat. Commun.*, 2020, **11**, 357.
39 A. Yousefi, A. Nezamzadeh-Ejhieh and M. Mirmohammadi, *Environ. Technol. Innovation*, 2021, **22**, 101496.
40 H. Derikvandi and A. Nezamzadeh-Ejhieh, *J. Hazard. Mater.*, 2017, **321**, 629–638.
41 A. Nezamzadeh-Ejhieh and A. Shirzadi, *Chemosphere*, 2014, **107**, 136–144.
42 N. Arabpour and A. Nezamzadeh-Ejhieh, *Process Saf. Environ. Prot.*, 2016, **102**, 431–440.
43 S. Vahabirad and A. Nezamzadeh-Ejhieh, *J. Solid State Chem.*, 2022, **310**, 123018.
44 N. Mehrabanpour, A. Nezamzadeh-Ejhieh, S. Ghattavi and A. Ershadi, *Appl. Surf. Sci.*, 2023, **614**, 156252.
45 N. Omrani and A. Nezamzadeh-Ejhieh, *Iran. J. Catal.*, 2025, **15**, 152515.
46 G. L. Semenza, *Annu. Rev. Pathol.: Mech. Dis.*, 2014, **9**, 47–71.
47 D. M. Gilkes, G. L. Semenza and D. Wirtz, *Nat. Rev. Cancer*, 2014, **14**, 430–439.
48 C. Donato, L. Kunz, F. Castro-Giner, A. Paasinen-Sohns, K. Strittmatter, B. M. Szczerba, R. Scherrer, N. Di Maggio, W. Heusermann, O. Biehlmaier, C. Beisel, M. Vetter, C. Rochlitz, W. P. Weber, A. Banfi, T. Schroeder and N. Aceto, *Cell Rep.*, 2020, **32**, 108105.
49 X. Jing, F. Yang, C. Shao, K. Wei, M. Xie, H. Shen and Y. Shu, *Mol. Cancer*, 2019, **18**, 157.
50 S. I. Gundersen and A. F. Palmer, *Biotechnol. Prog.*, 2008, **24**, 1353–1364.
51 Z. Yu, P. Zhou, W. Pan, N. Li and B. Tang, *Nat. Commun.*, 2018, **9**, 5044.
52 L. Sun, J.-e. Zhou, T. Luo, J. Wang, L. Kang, Y. Wang, S. Luo, Z. Wang, Z. Zhou, J. Zhu, J. Yu, L. Yu and Z. Yan, *Adv. Mater.*, 2022, **34**, 2109969.
53 S. Zeng, J. Chen, R. Gao, R. Chen, Q. Xue, Y. Ren, L. Liu, C. Tang, H. Hu, N. Zeng, S. Wen, H. Zhang, C. Liu and C. Fang, *Adv. Mater.*, 2024, **36**, 2308780.
54 J. Gao, H. Qin, F. Wang, L. Liu, H. Tian, H. Wang, S. Wang, J. Ou, Y. Ye, F. Peng and Y. Tu, *Nat. Commun.*, 2023, **14**, 4867.
55 J. Huang, L. Zhang, J. Zheng, Y. Lin, X. Leng, C. Wang, P. Li and L. Feng, *Biomaterials*, 2023, **299**, 122181.
56 X. Chen, B. B. Mendes, Y. Zhuang, J. Conniot, S. Mercado Argandona, F. Melle, D. P. Sousa, D. Perl, A. Chivu, H. K. Patra, W. Shepard, J. Conde and D. Fairen-Jimenez, *J. Am. Chem. Soc.*, 2024, **146**, 1644–1656.
57 J. Chen, H. Luo, Y. Liu, W. Zhang, H. Li, T. Luo, K. Zhang, Y. Zhao and J. Liu, *ACS Nano*, 2017, **11**, 12849–12862.
58 S. Azimi and A. Nezamzadeh-Ejhieh, *J. Mol. Catal. A: Chem.*, 2015, **408**, 152–160.
59 Z. Khodami and A. Nezamzadeh-Ejhieh, *J. Mol. Catal. A: Chem.*, 2015, **409**, 59–68.
60 M. Amiri and A. Nezamzadeh-Ejhieh, *Mater. Sci. Semicond. Process.*, 2015, **31**, 501–508.
61 Y. Li, P. Sun, L. Zhao, X. Yan, D. K. P. Ng and P.-C. Lo, *Angew. Chem., Int. Ed.*, 2020, **59**, 23228–23238.
62 J. Kim, H. R. Cho, H. Jeon, D. Kim, C. Song, N. Lee, S. H. Choi and T. Hyeon, *J. Am. Chem. Soc.*, 2017, **139**, 10992–10995.
63 W. Wu, Y. Pu, B. Zhou, Y. Shen, S. Gao, M. Zhou and J. Shi, *J. Am. Chem. Soc.*, 2022, **144**, 19038–19050.
64 Y. Li, Z. Du, Y. Zhang, X. Kang, J. Song, X. Chen, Y. Hu, Z. Yang, J. Qi and X. Shen, *Adv. Funct. Mater.*, 2024, **34**, 2315127.
65 C. Liu, M. Li, P. Li, Y. Bai, J. Pang, L. Fan and W. Tian, *Adv. Funct. Mater.*, 2021, **31**, 2105837.
66 W. Shen, T. Hu, X. Liu, J. Zha, F. Meng, Z. Wu, Z. Cui, Y. Yang, H. Li, Q. Zhang, L. Gu, R. Liang and C. Tan, *Nat. Commun.*, 2022, **13**, 3384.
67 W.-Q. Huang, F. Wang, A.-Z. Shen, L. Zhang, X. Nie, Z. Zhang, G. Chen, L. Xia, L.-H. Wang, S.-G. Ding, Q.-Y. Meng, W.-J. Zhang, C.-Y. Hong and Y.-Z. You, *Mater. Horiz.*, 2021, **8**, 597–605.
68 X. Zhou, M. You, F. Wang, Z. Wang, X. Gao, C. Jing, J. Liu, M. Guo, J. Li, A. Luo, H. Liu, Z. Liu and C. Chen, *Adv. Mater.*, 2021, **33**, 2100556.
69 Y. He, C. Cong, Y. He, Z. Hao, C. Li, S. Wang, Q. Zhao, H. He, R. Zhu, X. Li and D. Gao, *Chem. Eng. J.*, 2019, **375**, 122079.
70 J. Gan, J. Lei, Y. Li, M. Lu, X. Yu and G. Yu, *J. Am. Chem. Soc.*, 2024, **146**, 32689–32700.
71 X. Song, J. Xu, C. Liang, Y. Chao, Q. Jin, C. Wang, M. Chen and Z. Liu, *Nano Lett.*, 2018, **18**, 6360–6368.
72 Y. Deng, S. Huang, G. Jiang, L. Zhou, A. Nezamzadeh-Ejhieh, J. Liu and Z. Zhou, *RSC Med. Chem.*, 2024, **15**, 2996–3016.
73 C. Jiang, W. Li, J. Yan, X. Yu, Y. Feng, B. Li, Y. Liu and Y. Dai, *Adv. Healthcare Mater.*, 2024, **13**, 2401502.
74 C. Liu, Y. Cao, Y. Cheng, D. Wang, T. Xu, L. Su, X. Zhang and H. Dong, *Nat. Commun.*, 2020, **11**, 1735.
75 H. Yu, Y. Cheng, C. Wen, Y.-Q. Sun and X.-B. Yin, *Biomaterials*, 2022, **280**, 121308.
76 M. Huo, L. Wang, L. Zhang, C. Wei, Y. Chen and J. Shi, *Angew. Chem., Int. Ed.*, 2020, **59**, 1906–1913.
77 M. Li, Y. Shao, J. H. Kim, Z. Pu, X. Zhao, H. Huang, T. Xiong, Y. Kang, G. Li, K. Shao, J. Fan, J. W. Foley, J. S. Kim and X. Peng, *J. Am. Chem. Soc.*, 2020, **142**, 5380–5388.
78 Y. Zhao, M. Zhang, B. Lv, G. Xue, H. Jiang, G. Chen, Y. Ma, Y. Sun and J. Cao, *ACS Nano*, 2023, **17**, 21170–21181.
79 S. Li, F. Yang, Y. Wang, L. Jia and X. Hou, *Mater. Horiz.*, 2023, **10**, 5734–5752.
80 J. Dulak, J. Deshane, A. Jozkowicz and A. Agarwal, *Circulation*, 2008, **117**, 231–241.

81 T. T. Tien Vo, Q. C. Vo, V. P. Tuan, Y. Wee, H.-C. Cheng and I. T. Lee, *Redox Biol.*, 2021, **46**, 102124.
82 Y. Zhou, W. Yu, J. Cao and H. Gao, *Biomaterials*, 2020, **255**, 120193.
83 E. Jung, S.-H. Koh, M. Yoo and Y. K. Choi, *Int. J. Mol. Sci.*, 2020, **21**, 2273.
84 H.-H. Kim and S. Choi, *Int. J. Mol. Sci.*, 2018, **19**, 2381.
85 M. Ruopp, S. Reiländer, D. Haas, I. Caruana, D. Kronenberg, W. Schmehl, R. Stange and L. Meinel, *J. Controlled Release*, 2023, **357**, 299–308.
86 Q. Cui, X.-L. Liang, J.-Q. Wang, J.-Y. Zhang and Z.-S. Chen, *Biochem. Pharmacol.*, 2022, **201**, 115061.
87 S. W. Ryter, K. C. Ma and A. M. K. Choi, *Am. J. Physiol.: Cell Physiol.*, 2017, **314**, C211–C227.
88 B. Kawahara, S. Ramadoss, G. Chaudhuri, C. Janzen, S. Sen and P. K. Mascharak, *J. Inorg. Biochem.*, 2019, **191**, 29–39.
89 C. Xiao, Y. Sun, J. Fan, W. Nguyen, S. Chen, Y. Long, W. Chen, A. Zhu and B. Liu, *Acta Pharm. Sin. B*, 2023, **13**, 4591–4606.
90 C. Lv, Q. Su, J. Fang and H. Yin, *Biochem. Biophys. Res. Commun.*, 2019, **520**, 320–326.
91 J. Fang, R. Islam, W. Islam, H. Yin, V. Subr, T. Etrych, K. Ulbrich and H. Maeda, *Pharmaceutics*, 2019, **11**, 343.
92 R. Motterlini, J. E. Clark, R. Foresti, P. Sarathchandra, B. E. Mann and C. J. Green, *Circ. Res.*, 2002, **90**, e17–e24.
93 D. Zhang, Z. Lin, Y. Zheng, J. Song, J. Li, Y. Zeng and X. Liu, *ACS Nano*, 2020, **14**, 8985–8999.
94 Y. Opoku-Damoah, R. Zhang, H. T. Ta and Z. P. Xu, *Biomater. Sci.*, 2021, **9**, 6086–6097.
95 H. Yan, J. Du, S. Zhu, G. Nie, H. Zhang, Z. Gu and Y. Zhao, *Small*, 2019, **15**, 1904382.
96 X. Ji, C. Zhou, K. Ji, R. E. Aghoghovbia, Z. Pan, V. Chittavong, B. Ke and B. Wang, *Angew. Chem., Int. Ed.*, 2016, **55**, 15846–15851.
97 W. Tang, W. Fan, Z. Wang, W. Zhang, S. Zhou, Y. Liu, Z. Yang, E. Shao, G. Zhang, O. Jacobson, L. Shan, R. Tian, S. Cheng, L. Lin, Y. Dai, Z. Shen, G. Niu, J. Xie and X. Chen, *ACS Nano*, 2018, **12**, 12269–12283.
98 P. Sun, X. Jiang, B. Sun, H. Wang, J. Li, Q. Fan and W. Huang, *Biomaterials*, 2022, **280**, 121319.
99 H. Zhong, G. Chen, T. Li, J. Huang, M. Lin, B. Li, Z. Xiao and X. Shuai, *Nano Lett.*, 2023, **23**, 5083–5091.
100 Y. Li, Y. Pan, C. Chen, Z. Li, S. Du, X. Luan, Y. Gao, X. Han and Y. Song, *Small*, 2022, **18**, 2204244.
101 C. Tang, P. Ling, X. Gao, Q. Zhang, P. Yang, L. Wang, W. Xu and F. Gao, *ACS Biomater. Sci. Eng.*, 2024, **10**, 4009–4017.
102 B. Liu, X. Zhang, J. Li, S. Yao, Y. Lu, B. Cao and Z. Liu, *ACS Appl. Mater. Interfaces*, 2022, **14**, 7636–7645.
103 Y. Sun, C. An, L. Wu, W. Zeng, J. Wang, Y. Wang, J. He, G. Gao and D. Ye, *ACS Nano*, 2021, **15**, 16298–16313.
104 G. Ma, Z. Liu, C. Zhu, H. Chen, R. T. K. Kwok, P. Zhang, B. Z. Tang, L. Cai and P. Gong, *Angew. Chem., Int. Ed.*, 2022, **61**, e202207213.
105 X.-S. Wang, J.-Y. Zeng, M.-J. Li, Q.-R. Li, F. Gao and X.-Z. Zhang, *ACS Nano*, 2020, **14**, 9848–9860.
106 J. Lu, F. Chen, X. Xie, Z. Wu, Y. Chen, Y. Zhang, H. Fang, F. Ruan, D. Shao, Z. Wang and R. Pei, *Biomaterials*, 2023, **302**, 122313.
107 J. Zhu, A. Ouyang, J. He, J. Xie, S. Banerjee, Q. Zhang and P. Zhang, *Chem. Commun.*, 2022, **58**, 3314–3317.
108 A. Liu, Z. Huang, X. Du, N. Duvva, Y. Du, Z. Teng, Z. Liao, C. Liu, H. Tian and S. Huo, *Adv. Sci.*, 2024, **11**, 2403795.
109 W.-N. Zhao, M. Wang, C. Zhang, S. Sun and Y. Xu, *Chem. Commun.*, 2022, **58**, 8512–8515.
110 Q. Min, Z. Ni, M. You, M. Liu, Z. Zhou, H. Ke and X. Ji, *Angew. Chem., Int. Ed.*, 2022, **61**, e202200974.
111 Z. Li, Y. Wang, M. Liu, Y. Pan, Z. Ni, Q. Min, B. Wang, H. Ke and X. Ji, *J. Med. Chem.*, 2023, **66**, 14583–14596.
112 S. Cui, Y. Pan, C. Ma, B. Qi, Q. Min, M. Li, H. Chen, H. Ke and X. Ji, *Sci. China:Chem.*, 2025, **68**, 2565–2571.
113 W. Guo, S. Huang, J. An, J. Zhang, F. Dong, J. Dang and J. Zhang, *ACS Appl. Mater. Interfaces*, 2022, **14**, 50664–50676.
114 D.-W. Zheng, B. Li, C.-X. Li, L. Xu, J.-X. Fan, Q. Lei and X.-Z. Zhang, *Adv. Mater.*, 2017, **29**, 1703822.
115 S.-B. Wang, C. Zhang, Z.-X. Chen, J.-J. Ye, S.-Y. Peng, L. Rong, C.-J. Liu and X.-Z. Zhang, *ACS Nano*, 2019, **13**, 5523–5532.
116 X. Xiao, S. Liang, Y. Zhao, M. Pang, P. a. Ma, Z. Cheng and J. Lin, *Biomaterials*, 2021, **277**, 121120.
117 Q. Wang, Z. He, R. Zhang, J. Du, L. Zhu, X. Li, H. Yang, Y. Miao and Y. Li, *Chem. Eng. J.*, 2024, **480**, 148269.
118 M. Yuan, L. Yang, Z. Yang, Z. Ma, J. Ma, Z. Liu, P. a. Ma, Z. Cheng, A. Maleki and J. Lin, *Adv. Sci.*, 2024, **11**, 2308546.
119 T. Zhang, Q. Zheng, J. Huang and X. Li, *Adv. Funct. Mater.*, 2024, **34**, 2311029.
120 V. Calabrese, C. Mancuso, M. Calvani, E. Rizzarelli, D. A. Butterfield and A. M. Giuffrida Stella, *Nat. Rev. Neurosci.*, 2007, **8**, 766–775.
121 J. Park, K. Jin, A. Sahasrabudhe, P.-H. Chiang, J. H. Maalouf, F. Koehler, D. Rosenfeld, S. Rao, T. Tanaka, T. Khudiyev, Z. J. Schiffer, Y. Fink, O. Yizhar, K. Manthiram and P. Anikeeva, *Nat. Nanotechnol.*, 2020, **15**, 690–697.
122 B. N. Gantner, K. M. LaFond and M. G. Bonini, *Redox Biol.*, 2020, **34**, 101550.
123 C.-Y. Li, G. Anuraga, C.-P. Chang, T.-Y. Weng, H.-P. Hsu, H. D. K. Ta, P.-F. Su, P.-H. Chiu, S.-J. Yang, F.-W. Chen, P.-H. Ye, C.-Y. Wang and M.-D. Lai, *J. Exp. Clin. Cancer Res.*, 2023, **42**, 22.
124 U. Förstermann and W. C. Sessa, *Eur. Heart J.*, 2012, **33**, 829–837.
125 S. Mocellin, V. Bronte and D. Nitti, *Med. Res. Rev.*, 2007, **27**, 317–352.
126 Z. Zhao, X. Shan, H. Zhang, X. Shi, P. Huang, J. Sun, Z. He, C. Luo and S. Zhang, *J. Controlled Release*, 2023, **362**, 151–169.
127 J. Kim and S. N. Thomas, *Pharmacol. Rev.*, 2022, **74**, 1146–1175.
128 P. Gong, K. Zhao, X. Liu, C. Li, B. Liu, L. Hu, D. Shen, D. Wang and Z. Liu, *ACS Appl. Mater. Interfaces*, 2022, **14**, 46201–46211.

129 Y. Cheng, X. Jiao, Z. Wang, O. Jacobson, M. A. Aronova, Y. Ma, L. He, Y. Liu, W. Tang, L. Deng, J. Zou, Z. Yang, M. Zhang, Y. Wen, W. Fan and X. Chen, *Biomater. Sci.*, 2021, **9**, 2584–2597.
130 H. Lu, B. Liang, A. Hu, H. Zhou, C. Jia, A. Aji, Q. Chen, Y. Ma, W. Cui, L. Jiang and J. Dong, *Adv. Mater.*, 2025, **37**, 2412655.
131 Y. Cao, M. Liu, J. Cheng, J. Yin, C. Huang, H. Cui, X. Zhang and G. Zhao, *ACS Appl. Mater. Interfaces*, 2020, **12**, 28975–28984.
132 W. Jiang, W. Dong, M. Li, Z. Guo, Q. Wang, Y. Liu, Y. Bi, H. Zhou and Y. Wang, *ACS Nano*, 2022, **16**, 3881–3894.
133 K. Qiao, Y. Pan, S. Zhang, G. Shi, J. Yang, Z. Zhang, K. Wang, X. Chen and S. Ning, *ACS Nano*, 2024, **18**, 29689–29703.
134 Y. Wang, X. Yang, X. Chen, X. Wang, Y. Wang, H. Wang, Z. Chen, D. Cao, L. Yu and J. Ding, *Adv. Funct. Mater.*, 2022, **32**, 2206554.
135 X. Wan, T. Zheng, D. Wang, W. Pan, Y. Gao, N. Li and B. Tang, *Chem. Commun.*, 2022, **58**, 11803–11806.
136 X. Wu, Y. Cheng, R. Zheng, K. Xu, J. Yan, P. Song, Y. Wang, A. Rauf, Y. Pan and H. Zhang, *ACS Appl. Mater. Interfaces*, 2021, **13**, 19825–19835.
137 Y. Liu, X. Wang, J. Li, J. Tang, B. Li, Y. Zhang, N. Gu and F. Yang, *Adv. Mater.*, 2021, **33**, 2101701.
138 Y.-C. Sung, P.-R. Jin, L.-A. Chu, F.-F. Hsu, M.-R. Wang, C.-C. Chang, S.-J. Chiou, J. T. Qiu, D.-Y. Gao, C.-C. Lin, Y.-S. Chen, Y.-C. Hsu, J. Wang, F.-N. Wang, P.-L. Yu, A.-S. Chiang, A. Y.-T. Wu, J. J.-S. Ko, C. P.-K. Lai, T.-T. Lu and Y. Chen, *Nat. Nanotechnol.*, 2019, **14**, 1160–1169.
139 H.-Z. Yang, Y. Hu, J.-J. Chen, R.-M. Zhao, L. Pu, X.-Q. Yu and J. Zhang, *J. Drug Delivery Sci. Technol.*, 2024, **92**, 105296.
140 X. Fang, S. Cai, M. Wang, Z. Chen, C. Lu and H. Yang, *Angew. Chem., Int. Ed.*, 2021, **60**, 7046–7050.
141 L. Jiang, D. Chen, Z. Jin, C. Xia, Q. Xu, M. Fan, Y. Dai, J. Liu, Y. Li and Q. He, *Bioact. Mater.*, 2022, **12**, 303–313.
142 B. Li, P. Ji, S.-Y. Peng, P. Pan, D.-W. Zheng, C.-X. Li, Y.-X. Sun and X.-Z. Zhang, *Adv. Mater.*, 2020, **32**, 2000376.
143 S. Yao, M. Zheng, Z. Wang, Y. Zhao, S. Wang, Z. Liu, Z. Li, Y. Guan, Z. L. Wang and L. Li, *Adv. Mater.*, 2022, **34**, 2205881.
144 H. Zhang, X.-T. Tian, Y. Shang, Y.-H. Li and X.-B. Yin, *ACS Appl. Mater. Interfaces*, 2018, **10**, 28390–28398.
145 R. Jin, J. Xie, X. Yang, Y. Tian, P. Yuan, Y. Bai, S. Liu, B. Cai and X. Chen, *Biomater. Sci.*, 2020, **8**, 1865–1874.
146 Z. Fang, J. Zhang, Z. Shi, L. Wang, Y. Liu, J. Wang, J. Jiang, D. Yang, H. Bai, B. Peng, H. Wang, X. Huang, J. Li, L. Li and W. Huang, *Adv. Mater.*, 2023, **35**, 2301901.
147 M. Wang, Z. Hou, S. Liu, S. Liang, B. Ding, Y. Zhao, M. Chang, G. Han, A. A. A. Kheraif and J. Lin, *Small*, 2021, **17**, 2005728.
148 L. Wang, Y. Tian, K. Lai, Y. Liu, Y. Liu, J. Mou, S. Yang and H. Wu, *ACS Biomater. Sci. Eng.*, 2023, **9**, 797–808.
149 S. Li, X. Song, W. Zhu, Y. Chen, R. Zhu, L. Wang, X. Chen, J. Song and H. Yang, *ACS Appl. Mater. Interfaces*, 2020, **12**, 30066–30076.
150 S. Wang, Y. Wang, J. Lv, C. Xu, Y. Wei, G. Wang and M. Li, *Adv. Healthcare Mater.*, 2024, **13**, 2303579.
151 Y. Zheng, Y. Liu, F. Wei, H. Xiao, J. Mou, H. Wu and S. Yang, *Acta Biomater.*, 2021, **121**, 592–604.
152 M. Dole, F. R. Wilson and W. P. Fife, *Science*, 1975, **190**, 152–154.
153 P. Luo, H. Wang, X. Wen, X. Luo and P. Xu, *Adv. Energy Mater.*, 2024, **14**, 2302532.
154 P. Zhao, Z. Jin, Q. Chen, T. Yang, D. Chen, J. Meng, X. Lu, Z. Gu and Q. He, *Nat. Commun.*, 2018, **9**, 4241.
155 J. Chen, S. Lin, D. Zhao, L. Guan, Y. Hu, Y. Wang, K. Lin and Y. Zhu, *Adv. Funct. Mater.*, 2021, **31**, 2006853.
156 R. Sun, X. Liu, G. Li, H. Wang, Y. Luo, G. Huang, X. Wang, G. Zeng, Z. Liu and S. Wu, *ACS Nano*, 2020, **14**, 8135–8148.
157 B. Zhao, Y. Wang, X. Yao, D. Chen, M. Fan, Z. Jin and Q. He, *Nat. Commun.*, 2021, **12**, 1345.
158 Y. Xu, M. Fan, W. Yang, Y. Xiao, L. Zeng, X. Wu, Q. Xu, C. Su and Q. He, *Adv. Mater.*, 2021, **33**, 2101455.
159 Q. Shi, T. Yin, C. Zeng, H. Pan, Z. Chen, L. Wang, B. Wang, M. Zheng and L. Cai, *Bioact. Mater.*, 2024, **37**, 505–516.
160 Y. Zhang, X. Deng, L. Xia, J. Liang, M. Chen, X. Xu, W. Chen, J. Ding, C. Yu, L. Liu, Y. Xiang, Y. Lin, F. Duan, W. Feng, Y. Chen and X. Gao, *Adv. Sci.*, 2025, **12**, 2408807.
161 Y. Wu, L. Su, M. Yuan, T. Chen, J. Ye, Y. Jiang, J. Song and H. Yang, *Angew. Chem., Int. Ed.*, 2021, **60**, 12868–12875.
162 M. Yuan, S. Liang, L. Yang, F. Li, B. Liu, C. Yang, Z. Yang, Y. Bian, P. a. Ma, Z. Cheng and J. Lin, *Adv. Mater.*, 2023, **35**, 2209589.
163 G. Qi, B. Wang, X. Song, H. Li and Y. Jin, *Natl. Sci. Rev.*, 2020, **7**, 660–670.
164 G. Qi, T. Yu, J. Li, Z. Guo, K. Ma and Y. Jin, *Adv. Mater.*, 2023, **35**, 2208414.
165 N. Yang, F. Gong, B. Liu, Y. Hao, Y. Chao, H. Lei, X. Yang, Y. Gong, X. Wang, Z. Liu and L. Cheng, *Nat. Commun.*, 2022, **13**, 2336.
166 X. Meng, Z. Liu, L. Deng, Y. Yang, Y. Zhu, X. Sun, Y. Hao, Y. He and J. Fu, *Adv. Sci.*, 2024, **11**, 2401269.
167 J. Yang, G. Li, J. Yuan, S. Jing, X. Wang, F. Yang, Y. Liu, Y. Ding, G. Li, G. Xie, A. Tao, M. Liu and M. Xie, *Adv. Funct. Mater.*, 2022, **32**, 2206406.
168 W. Liu, M. Guo, Y. Hu, Y. Chen, Y. Wang, A. Nezamzadeh-Ejhieh, H. Li, C. Lu and J. Liu, *Eur. J. Med. Chem.*, 2025, **288**, 117427.
169 M. Guo, Y. Jian, J. Chen, Y. Zhang, A. Nezamzadeh-Ejhieh, X. Deng, Y. Xue, Y. Peng, C. Lu and J. Liu, *Mater. Today Chem.*, 2025, **45**, 102627.
170 P. Gao, M. Wang, Y. Chen, W. Pan, P. Zhou, X. Wan, N. Li and B. Tang, *Chem. Sci.*, 2020, **11**, 6882–6888.
171 X. Du, K. He, X. Jiang, S. Chen, R. Zhang, P. Sun and Q. Fan, *ACS Appl. Polym. Mater.*, 2022, **4**, 5103–5112.
172 N. Mahhengam, K. Kazemnezhad, H. Setia Budi, M. J. Ansari, D. Olegovich Bokov, W. Suksatan, L. Thangavelu and H. Siahmansouri, *J. Drug Targeting*, 2022, **30**, 494–510.
173 Z. Yu, M. Wang, W. Pan, H. Wang, N. Li and B. Tang, *Chem. Sci.*, 2017, **8**, 4896–4903.

174 C. Rao, D. Liao, Y. Pan, Y. Zhong, W. Zhang, Q. Ouyang, A. Nezamzadeh-Ejhieh and J. Liu, *Expert Opin. Drug Delivery*, 2022, **19**, 1183–1202.
175 J. Chen, Z. Zhang, J. Ma, A. Nezamzadeh-Ejhieh, C. Lu, Y. Pan, J. Liu and Z. Bai, *Dalton Trans.*, 2023, **52**, 6226–6238.
176 D. Liao, J. Huang, C. Jiang, L. Zhou, M. Zheng, A. Nezamzadeh-Ejhieh, N. Qi, C. Lu and J. Liu, *Pharmaceutics*, 2023, **15**, 2071.
177 M. Li, Z. Zhang, Y. Yu, H. Yuan, A. Nezamzadeh-Ejhieh, J. Liu, Y. Pan and Q. Lan, *Mater. Adv.*, 2023, **4**, 5050–5093.
178 Y. Zeng, D. Liao, X. Kong, Q. Huang, M. Zhong, J. Liu, A. Nezamzadeh-Ejhieh, Y. Pan and H. Song, *Colloids Surf., B*, 2023, **232**, 113612.
179 Z. Luo, Y. Sheng, C. Jiang, Y. Pan, X. Wang, A. Nezamzadeh-Ejhieh, J. Ouyang, C. Lu and J. Liu, *Dalton Trans.*, 2023, **52**, 17601–17622.
180 J. Ma, Z. Chen, Y. Diao, M. Ye, X. Liu, S. Cui, M. Zhong, A. Nezamzadeh-Ejhieh, J. Liu and J. Ouyang, *React. Funct. Polym.*, 2024, **200**, 105918.
181 J. Yu, W. Chen, L. Qin, A. Nezamzadeh-Ejhieh, F. Cheng, W. Liu, J. Liu and Z. Bai, *J. Mol. Struct.*, 2025, **1321**, 139984.
182 Z. Zhu, Q. Ouyang, L. Zhou, C. Fan, M. Zheng, A. Nezamzadeh-Ejhieh, H. Yuan, Y. Peng and J. Liu, *J. Mol. Struct.*, 2025, **1321**, 139797.
183 J. Li, S. Yin, L. Zhou, A. Nezamzadeh-Ejhieh, Y. Pan, L. Qiu, J. Liu and Z. Zhou, *Biomater. Sci.*, 2024, **12**, 5912–5932.
184 Y. Zeng, G. Xu, X. Kong, G. Ye, J. Guo, C. Lu, A. Nezamzadeh-Ejhieh, M. Shahnawaz Khan, J. Liu and Y. Peng, *Int. J. Pharm.*, 2022, **627**, 122228.
185 X. Wan, J. Yin, Q. Yan, H. Hu, T. Zheng, Y. Chai, W. Pan, Y. Gao, N. Li and B. Tang, *Chem. Commun.*, 2022, **58**, 5877–5880.
186 N. Omrani and A. Nezamzadeh-Ejhieh, *Sep. Purif. Technol.*, 2020, **235**, 116228.
187 S. A. Mirsalari and A. Nezamzadeh-Ejhieh, *Sep. Purif. Technol.*, 2020, **250**, 117235.
188 S. Ghattavi and A. Nezamzadeh-Ejhieh, *Composites, Part B*, 2020, **183**, 107712.
189 P. Hemmatpour and A. Nezamzadeh-Ejhieh, *Chemosphere*, 2022, **307**, 135925.